อุณหภูมิการเปลี่ยนสถานะของโลหะเซอร์โคเนียมจากวิธีพลศาสตร์เชิงโมเลกุลแบบเดิม

นายพรจักร ศรีพัชราวุธ

วิทยานิพนธ์นี้เป็นส่วนหนึ่งของการศึกษาตามหลักสูตรปริญญาวิทยาศาสตรมหาบัณฑิต
สาขาวิชาฟิสิกส์ ภาควิชาฟิสิกส์
คณะวิทยาศาสตร์ จุฬาลงกรณ์มหาวิทยาลัย
ปีการศึกษา 2546

ISBN 974-17-3558-8

THE PHASE TRANSITION TEMPERATURE IN ZIRCONIUM METAL FROM THE CLASSICAL MOLECULAR DYNAMICS METHOD

Mr. Pornjuk Srepusharawoot

A Thesis Submitted in Partial Fulfillment of the Requirements
for the Degree of Master of Science in Physics
Department of Physics
Faculty of Science
Chulalongkorn University
Academic Year 2003

ISBN 974-17-3558-8

Thesis Title	The Phase Transition Temperature in Zirconium Metal from the Classical Molecular Dynamics Method
By	Pornjuk Srepusharawoot
Field of Study	Physics
Thesis Advisor	Assistant Professor Dr. Udomsilp Pinsook

Accepted by the Faculty of Science, Chulalongkorn University in Partial Fulfillment of the Requirements for the Master's Degree

…….. Dean of Faculty of Science
(Associate Professor Wanchai Phothipichitr, Ph.D)

THESIS COMMITTEE

…….. Chairman
(Associate Professor David Ruffolo, Ph.D)

…….……. Thesis Advisor
(Assistant Professor Udomsilp Pinsook, Ph.D)

…….. Member
(Thiti Bovornrattanaraks, Ph.D)

…….. Member
(Somrit Wongmanerod, Ph.D)

นายพรจักร ศรีพัชราวุธ : อุณหภูมิการเปลี่ยนสถานะของโลหะเซอร์โคเนียมจากวิธีพลศาสตร์เชิงโมเลกุลแบบเดิม (THE PHASE TRANSITION TEMPERATURE IN ZIRCONIUM METAL FROM THE CLASSICAL MOLECULAR DYNAMICS METHOD) อ.ที่ปรึกษา: ผศ. ดร. อุดมศิลป์ ปิ่นสุข, จำนวนหน้า 66 หน้า. ISBN 974-17-3558-8.

พลังงานอิสระแบบเฮลม์โฮลซ์ถูกระบุเพื่ออธิบายการเปลี่ยนสถานะจากโครงสร้างแบบ body centered cubic (bcc) ไปยัง โครงสร้างแบบ hexagonal close packed (hcp) ในโลหะเซอร์โคเนียม ผู้วิจัยใช้วิธีพลศาสตร์เชิงโมเลกุลแบบเดิมในการคำนวณหาองค์ประกอบของพลังงานอิสระเฮล์มโฮลซ์ ได้แก่ พลังงานภายใน และ เอนโทรปีซึ่งประกอบด้วยเอนโทรปีเนื่องมาจากการสั่น และอิเล็กทรอนิกส์เอนโทรปี เอนโทรปีเนื่องจากการสั่นรวมผลของความเป็นฮาร์มอนิกส์ และ แอนฮาร์มอนิกส์ เอนโทรปีเนื่องจากการสั่นสามารถคำนวณโดยใช้ความหนาแน่นสถานะของโฟนอนซึ่งคำนวณมาจากvelocity autocorrelation function เอนโทรปีจากการสั่นแบบแอนฮารมอนิกส์สามารถคำนวณโดยใช้พลังงานอิสระแอนฮาร์มอนิกส์ อิเล็กทรอนิกส์เอนโทรปีถูกคำนวณมาจากความหนาแน่นสถานะแบบอิเล็กทรอนิกส์ ผู้วิจัยพบว่า ผลต่างของเอนโทรปีเนื่องมาจากการสั่นระหว่างสถานะแบบ bcc และ hcp ที่อุณหภูมิ 1135 เคลวิน มีค่า 0.20 k_B เปรียบเทียบกับ 0.26 k_B จากการทดลอง และ อุณหภูมิการเปลี่ยนสถานะมีค่า 1047±210 เคลวิน เปรียบเทียบกับ 1135 เคลวินจากการทดลอง ผลการจำลองจากวิธีพลศาสตร์เชิงโมเลกุลแบบเดิมมีค่าใกล้เคียงกับผลที่ได้จากการทดลอง

ภาควิชาฟิสิกส์ ลายมือชื่อนิสิต.....
สาขาวิชาฟิสิกส์ ลายมือชื่ออาจารย์ที่ปรึกษา.....
ปีการศึกษา 2546 ลายมือชื่ออาจารย์ที่ปรึกษาร่วม.....

4372341223 : MAJOR PHYSICS
KEY WORD: HELMHOLTZ FREE ENERGY / ENTROPY
PORNJUK SREPUSHARAWOOT : THE PHASE TRANSITION TEMPERATURE IN ZIRCONIUM METAL FROM THE CLASSICAL MOLECULAR DYNAMICS METHOD. THESIS ADVISOR : ASST. PROF. UDOMSILP PINSOOK, Ph.D., 66 pp. ISBN 974-17-3558-8

The Helmholtz free energy is determined in order to describe the bcc-hcp phase transition. We used the classical Molecular Dynamics method to evaluate the components of the Helmholtz free energy such as the internal energy and the entropy composed of the vibrational entropy and the electronic entropy. The vibrational entropy includes harmonic and anharmonic effects. The harmonic vibrational entropy is calculated from the phonon density of states, which comes from the velocity autocorrelation function. The anharmonic vibrational entropy can be calculated from the anharmonic free energy. The electronic entropy is evaluated from the electronic density of states. We found that the vibrational entropy difference between the bcc and the hcp phases at transition temperature is 0.20 k_B, compared with 0.26 k_B from experiments, and the transition temperature is 1047±210 K, compared with 1135 K from experiments. The results from classical Molecular Dynamics are in good agreement with the experimental results.

Department Physics Student's signature.....
Field of study Physics Advisor's signature.....
Academic year 2003 Co-advisor's signature.....

Acknowledgements

The author wishes to express his sincere appreciation and gratitude to his advisor Assistant Professor Dr. Udomsilp Pinsook for his valuable advice, discussions, helps and best Molecular Dynamics code. He wishes to express his gratitude to the thesis committee, Associate Professor Dr. David Ruffolo, Dr. Thiti Bovornrattanaraks and Dr. Somrit Wongmanerod for their reading and criticizing this manuscript.

Sincerely, he would like to thank Dr. Boonchoat Paosawatyanyong for providing computer facilities. He thanks Associate Professor Dr. Rajeev Ahuja for providing the electronic density of states data. He is indebted to Mr. Pairot Moontragoon, Mr. Apirath Phusittrakool and Mr. Kittipat Malakit for their advantageous suggestions in computer programming. Thanks go to all friends for their encouragement.

Finally, he would like to show invaluable appreciation to his parents, Mr.Boonsong and Mrs.Vilasinee Srepusharawoot for their warmest support.

Contents

Page

Contents (Cont.)

Page

List of Tables

Page

List of Figures

List of Figures (Cont.)

List of Figures (Cont.)

Chapter 1

Introduction

The bcc-hcp phase transition is one of the most frequently observed structural changes in many metals [7, 22, 46] and alloys [18, 39]. The bcc-hcp phase transition is an important phenomenon in material science as it can exhibit temperature hardening e.g., thermal expansion and shape memory effects in many materials. We choose zirconium as a representative because the transition mechanism is comparatively simple, i.e. driven by excess vibrational and electronic entropy [27, 28, 43]. Moreover, zirconium has no magnetic moment [42] so that the magnetic effects can be negligible. In the case of titanium and its alloys, the magnetic effects complicate the studies involving these materials.

Zirconium is a ductile, grayish-white, strong and lustrous metal. It was discovered by Klaproth, a German chemist, in 1789 and was isolated in 1824 by Berzelius. Zirconium is a transition metal in group IV. It has atomic weight which is 91.22 amu and the atomic number is 40. The electronic structure is

[Kr]$4d^2 5s^2$. The melting point of zirconium is 2125 K and the coefficient of thermal expansion is $5.89 \times 10^{-6} \mathrm{K}^{-1}$ which lower than titanium, iron and copper. Zirconium resists the attacking by strong acids except hydrofluoric. It is used for constructing highly corrosion resistant equipment. Zirconium has a very small neutron scattering cross section. Consequently, it is used in nuclear reactor for cladding the tubes in nuclear reactor. The density of zirconium is 6510 $\mathrm{kg/m}^3$ which lower than that of iron, stainless alloys and nickel. In addition, the thermal conductivity is 22 $\mathrm{W(mK)}^{-1}$ which higher than about 30 percent of stainless alloy. Zirconium is a nontoxic and biocompatible metal. It is suitable for making equipment used in food processing or medical equipment such as surgical tools.

Zirconium has a hexagonal close packed (hcp) structure at the temperature lower than the transition temperature. This is in agreement with the result of Ahuja *et al.* [37] which use *ab initio* method to confirm the stability of the hcp phase at absolute zero temperature. In addition, when the temperature is higher than the transition temperature, it has a body centered cubic (bcc) structure. The sensible transition temperature from various experiments is 1135 K [1, 2, 22]. The phase diagram of group IV transition metals including zirconium is shown in Fig (1.1). In this work, we are interested in the bcc-hcp phase only. The bcc-ω phase and the ω-hcp phase transitions are beyond our scope.

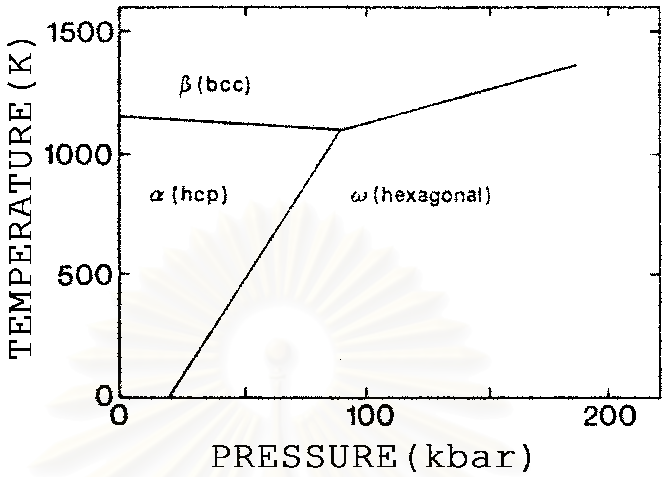

Fig. (1.1) Typical P-T diagram of group IV transition metals [23]

The studies of the effects of phonons on the bcc-hcp phase transition using Molecular Dynamics simulation is first suggested by Willaime and Massobrio [12, 13]. They used the tight binding scheme to construct an interatomic potential for zirconium. They found that the transition temperature is approximately 1912 K and the difference vibrational entropy, $\Delta S_{vib} = S_{bcc} - S_{hcp}$, is 0.143 ± 0.01 k_B/atom at the transition temperature. Salomon [9] used the same interatomic potential to calculated the free energy of the bcc and the hcp phases by performing Monte Carlo simulation. He found that the transition temperature is 1850 K and $\Delta S_{vib} = 0.126$ k_B/atom at 1200 K whereas the transition temperature and ΔS_{vib} from experiments are 1135 K and 0.26 k_B/atom [2, 19, 31] respectively. It is important to point out here that the experimental and the calculated transition temperature are not in good agreement. We believe that the cause of this dis-

agreement comes from neglecting the effects of the anharmonic and the electronic entropy.

Experimental results [22, 34] and many theoretical predictions [3, 14, 24] showed that the phonons in zirconium are strongly anharmonic. This was confirmed by *ab initio* works of Persson *et al.* [32] and Nishitani *et al.* [19], and molecular dynamics studies [12, 13, 40, 41, 42]. Evidentally, the anharmonic entropy is the important effects in zirconium. Furthermore, various theoretical works [26, 54] showed that even though the electronic structure has a minor effects, it cannot be neglected.

In this research, we improve the calculation of the transition temperature in zirconium by explicitly including the anharmonic and the electronic effects. The Classical Molecular Dynamics is an essential tool in this research. It is explained in chapter 2. In chapter 3, the harmonic vibrational entropy and the electronic entropy formulae are derived and the anharmonic vibrational entropy can be calculated from the anharmonic free energy [6]. The results of the vibrational entropy composes of the harmonic and the anharmonic parts and the electronic entropy are discussed in chapter 4. Finally, the conclusions of this research are in chapter 5.

Chapter 2

Molecular Dynamics

Molecular Dynamics (MD) is a powerful method for studying a classical many-body system. It produces the time evolution of a system of N particles by numerically solving the equations of motion. In this research, we use the classical Molecular Dynamics method to study the bcc-hcp phase transition in zirconium. The equations of motion obey Newton's second law and can be written as

$$m_i \frac{d^2 \vec{r}_i}{dt^2} = -\vec{\nabla}\phi_i \ , \tag{2.1}$$

where ϕ_i is a potential energy function corresponding with zirconium atom. ϕ_i depends only on the displacements between atoms (r_{ij}). $\vec{r}_i$ is the i^{th} atomic displacement. Conventionally, classical Molecular Dynamics simulations conserve both the total energy and the linear momentum. According to Eq. (2.1), accurate results can be obtained by imposing a good potential energy, a reasonable integration algorithm and suitable initial and boundary conditions. We discuss the potential energy in section (2.1), the initial and boundary conditions in sec-

tion (2.2), measuring pressure in section (2.3) and the integration algorithm in section (2.4).

2.1 The Potential Energy

In order to describe the properties of transition metals, we can construct a potential energy function which contains two essential parts which are the repulsive energy or Coulomb repulsion between two neighboring atoms and the attractive or bonding part. Hence the potential form can be written as

$$\phi = \phi_{rep} + \phi_{bond} \ ,$$

where ϕ_{rep} is the potential energy from the repulsive part. ϕ_{bond} is the potential energy from the bonding part which comes from the repulsion of neighboring atoms.

In this research, we use Finnis-Sinclair type interatomic potential which is assumed in a cubic spline form [17]. The potential was fitted in order to account for many body effects which are essential in transition metals. Both repulsive and bonding parts are short range. The potential energy of the i^{th} atom can be written as

$$\phi_i = \frac{1}{2}\sum_j V\left(r_{ij}\right) - \sqrt{\rho_i} \ , \tag{2.2}$$

where

$$V\left(r_{ij}\right)=\sum_{k=1}^{6}A_k\left(R_k-r_{ij}\right)^3H\left(R_k-r_{ij}\right)\ ,$$

and

$$\rho_i=\sum_{j}\sum_{k=1}^{2}a_k\left(r_k-r_{ij}\right)^3H\left(r_k-r_{ij}\right)\ ,$$

where $H(x)$ is the heaviside step function which is 0 where $x<0$ and 1 where $x\geq 0$. r_{ij} are the separation distance between atoms i and j. A_k, a_k, R_k, r_k are fitting parameters shown in Table 2.1.

k	A_k (eV/Å^3)	R_k(Å)	a_k(eV^2/Å^3)	r_k(Å)
1	-0.61248219	5.5763004	0.50569395	5.5763004
2	0.87645549	5.4848856	-0.00890725	4.7992749
3	-0.21947820	5.2106413	-	-
4	-0.01371379	4.3422011	-	-
5	0.68830444	3.6565904	-	-
6	1.45995293	3.1995166	-	-

Table 2.1: Fitting parameters of zirconium [16, 40]

The potential is fitted to some anisotropic properties such as the non-ideal c/a ratio, the cohesive energy of the hcp crystal structure relative to other possible structures, the energetic of vacancies and stacking faults. These properties are measured experimentally. This potential provides a good descriptions for both the bcc and hcp phases in zirconium [41, 42]. However, by using this potential at temperature lower than the transition temperature, zirconium can transform from the bcc to the hcp phase. This argument is confirmed by Figs. (2.1 - 2.2).

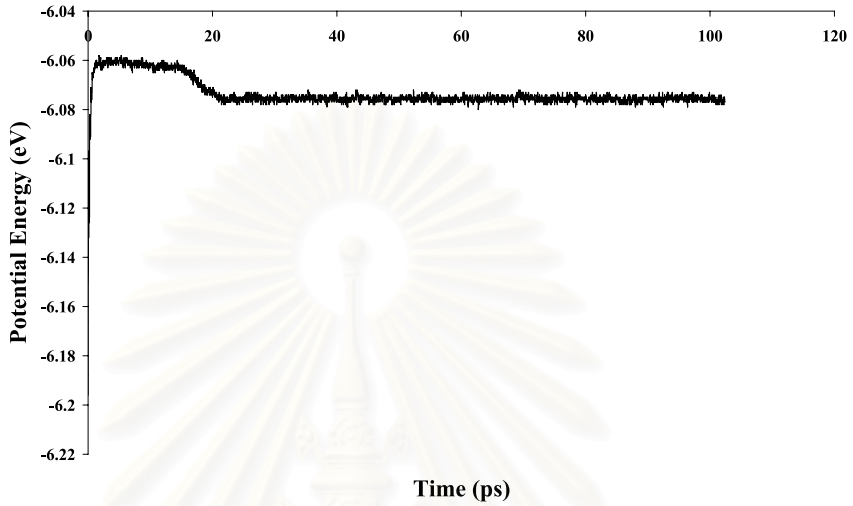

Fig. (2.1) The potential energy as a function of temperature from MD simulation for the bcc phase at T=1100 K

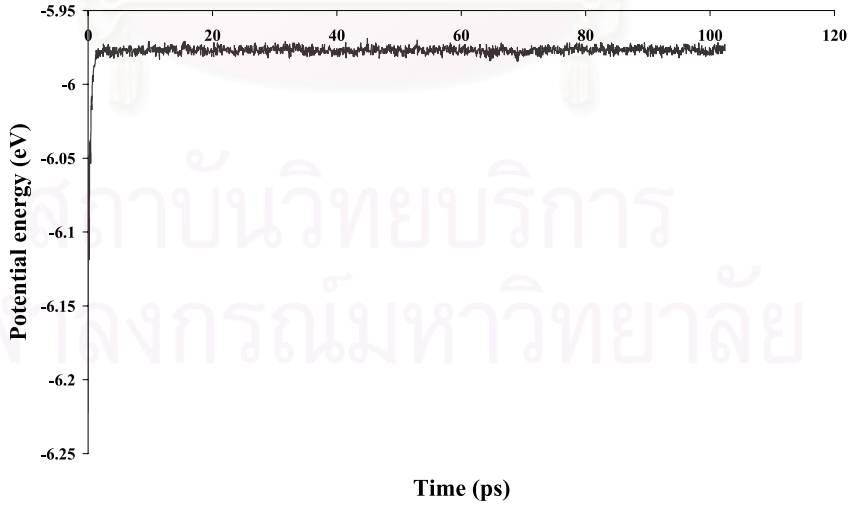

Fig. (2.2) The potential energy as a function of temperature from MD simulation for the hcp phase at T=1800 K

According to Fig. (2.1), if we start from the bcc phase, when the temperature is lower than the transition temperature, it induces the phase transition to the hcp phase. On the other hand, when the temperature is higher than the transition temperature, there are no transformation from the hcp to the bcc phase as shown in Fig. (2.2).

2.2 Initial and Boundary Conditions

In general MD simulations, we must solve a series of differential equations, i.e., Eq. (2.1) in order to obtain the position, the velocity and the acceleration of each atom at time t. The MD simulation is an initial value problems. Eq. (2.1) is a second-order ordinary differential equations. Thus mathematically Eq. (2.1) must satisfy two sets of initial conditions: specifying the initial coordinate and initial velocities. Firstly the atomic configuration can be set to the bcc or the hcp for zirconium at the starting time. Secondly, the kinetic energy of the system, which corresponds with the temperature T, is

$$\frac{1}{2}\sum_i m_i v_i^2 = \frac{3}{2}Nk_BT \ . \tag{2.3}$$

However, the choice of $\{\vec{v}_i\}$ is arbitrary and must conserved the linear momentum i.e. $\sum_i m_i\vec{v}_i = 0$. If we need to carry out some simulations which are compatible with experiments of temperature $T_{desired}$, without a priori reason, some procedures

must be followed. At the starting time, we simply randomize the velocity of each atom, i.e. $\vec{v}_i(0)$. Every velocity of each atom at this time will not satisfy Eq. (2.3), that is

$$\frac{1}{2}\sum_i m_i v_i^2(0) \neq \frac{3}{2}Nk_BT_{desired} \ .$$

In order to ensure Eq. (2.3), we introduce rescale velocity method. If the kinetic energy at starting time corresponding with the started temperature, T_{start}, i.e.

$$\frac{1}{2}\sum_i m_i v_i^2(0) = \frac{3}{2}Nk_BT_{start} \ ,$$

then we can rescale the velocity by multiplying them with some constant value, called "rescaling factor" (α) . The rescaling factor is defined as

$$\alpha = \sqrt{\frac{T_{desired}}{T_{start}}} \ , \tag{2.4}$$

so that

$$\alpha^2 \sum_i \frac{1}{2} m_i v_i^2(0) = \frac{3}{2}Nk_BT_{desired} \ . \tag{2.5}$$

Now we can rescale the velocity corresponding with the kinetic energy and the desired temperature. In our simulations, we rescale every 200 time steps. We do not rescale every time step because the system will be too constrained and natural evolution will be suppressed.

A finite number of atoms is contained in simulation box in our simulations. In contrast, in a real system, the number of atoms in a solid is very large.

Therefore the situation in the simulation is not realistic because the atoms near boundaries would have fewer neighbors than atoms inside. Then the effects of the surface of the simulation box become dominant. The surface effects can be reduced by periodic boundary conditions (PBC) [8]. The idea of PBC is that the particles or atoms in the solid can reenter the simulation box when they leave a box boundary from the opposite side. By using PBC, the surface effects are removed from the simulations.

2.3 Measuring Pressure

The measurement of the pressure in a MD simulation is based on Clausius virial function [8].

$$\mathrm{W}\left(r_1, ..., r_n\right) = \sum_{i=1}^{N} \vec{r}_i \cdot \vec{F}_i^{TOT} \ , \tag{2.6}$$

where $\vec{F}_i^{TOT}$ is the total force acting on i^{th} atom. The statistical average of $\mathrm{W}\left(r_1, ..., r_n\right)$ over the molecular dynamics trajectory is

$$\begin{aligned} \langle \mathrm{W} \rangle &= \lim_{t\to\infty} \frac{1}{t} \int_0^t \sum_{i=1}^{N} \vec{r}_i \cdot \vec{F}_i^{TOT} \, d\tau \ , \\ &= \lim_{t\to\infty} \frac{1}{t} \int_0^t \sum_{i=1}^{N} \vec{r}_i \cdot m_i \ddot{\vec{r}}_i \, d\tau \ . \end{aligned} \tag{2.7}$$

We integrate Eq. (2.7) by parts and get

$$\langle \mathrm{W} \rangle = - \lim_{t\to\infty} \frac{1}{t} \int_0^t \sum_{i=1}^{N} m_i |\dot{\vec{r}}_i|^2 \, d\tau \ . \tag{2.8}$$

This equation suggests that we can use the equipartition theorem [29] to calculate Eq. (2.8) . Then

$$\langle \mathrm{W} \rangle = -3Nk_BT \ .$$

From Eq. (2.6), we can write the average $\mathrm{W}(r_1, ..., r_n)$ as

$$\langle \mathrm{W} \rangle = \left\langle \sum_{i=1}^{N} \vec{r_i} \cdot \vec{F_i^{TOT}} \right\rangle = -3Nk_BT \ . \tag{2.9}$$

The total force acting on each particle is

$$\vec{F_i^{TOT}} = \vec{F_i^{int}} + \vec{F_i^{ext}} \ ,$$

where $\vec{F_i^{int}}$ is the internal force which comes from the interatomic interaction, and $\vec{F_i^{ext}}$ is the external force exerted by the simulation box or the container wall. Consequently, the Clausius virial function can be written as

$$\langle \mathrm{W} \rangle = \left\langle \sum_{i=1}^{N} \vec{r_i} \cdot \vec{F_i^{int}} \right\rangle + \left\langle \sum_{i=1}^{N} \vec{r_i} \cdot \vec{F_i^{ext}} \right\rangle \ . \tag{2.10}$$

Next, we want to calculate the external work. If the particles are enclosed in a parallelepiped container of side L_x, L_y, L_z, volume $V = L_xL_yL_z$ and using the coordinates origin on one of its corners, the second term of Eq. (2.10) is

$$< \mathrm{W}^{ext} >= \left\langle \sum_{i=1}^{N} \vec{r_i} \cdot \vec{F_i^{ext}} \right\rangle = L_x(-PL_yL_z) + L_y(-PL_xL_z) + L_z(-PL_xL_y) \ ,$$

$$= -3PV \ , \tag{2.11}$$

where $-PL_yL_z$ is the external force acting on yz wall. The minus sign comes from the direction of the external force acting on the yz wall. The same situation occurs in y and z directions. We substitute Eq. (2.9) and Eq. (2.11) into Eq. (2.10), so we get

$$\langle \mathrm{W} \rangle = \left\langle \sum_{i=1}^{N} \vec{r}_i \cdot \vec{F}_i^{int} \right\rangle - 3PV = -3Nk_BT \ ,$$

$$PV = Nk_BT + \frac{1}{3} \left\langle \sum_{i=1}^{N} \vec{r}_i \cdot \vec{F}_i^{int} \right\rangle \ , \tag{2.12}$$

We can notice that if the particles are non-interacting, i.e. the potential energy (ϕ) is zero, Eq. (2.12) is reduced to the well known equation of states of ideal gas. We can evaluate the pressure by

$$P = nk_BT + \frac{1}{3V} \left\langle \sum_{i=1}^{N} \vec{r}_i \cdot \vec{F}_i^{int} \right\rangle \ , \tag{2.13}$$

where n is the density of the particles, (N/V).

2.4 The Integration Algorithm

The important tool of MD is the integration algorithm. It is required to integrate the Newton equation of motions in order to obtain the position, the velocity, the acceleration of each particle at each time step. A good integration algorithm should produce accurate results, conserve total energy and momentum of the system and use less computing time. The fourth-order Gear predictor-corrector

algorithm is chosen because it has a simple form and it is reasonably fast. Press *et al.* [44] discuss that this algorithm is suitable for a problem which involves high-precision solutions of very smooth and complicated functions. The fourth order Gear predictor-corrector integration algorithm contains the prediction and the correction parts. In the prediction part, the position, the velocity and the acceleration at time $t+\delta t$ are estimated by using information at time t and Taylor expansions. This can be written in a matrix form as

$$\begin{pmatrix} r^p(t+\delta t) \\ \dot{r}^p(t+\delta t) \\ \ddot{r}^p(t+\delta t) \\ \dddot{r}^p(t+\delta t) \end{pmatrix} = \begin{pmatrix} 1 & \delta t & \frac{1}{2}\delta t^2 & \frac{1}{6}\delta t^3 \\ 0 & 1 & \delta t & \frac{1}{2}\delta t^2 \\ 0 & 0 & 1 & \delta t \\ 0 & 0 & 0 & 1 \end{pmatrix} \begin{pmatrix} r(t) \\ \dot{r}(t) \\ \ddot{r}(t) \\ \dddot{r}(t) \end{pmatrix} . \tag{2.14}$$

The superscript p denotes the prediction values. We can see that the interatomic force is not included at this time. In the next step, we calculate the difference between the predicted and corrected acceleration which is written as

$$\Delta\ddot{r}(t+\delta t) = \ddot{r}^c(t+\delta t) - \ddot{r}^p(t+\delta t) \ . \tag{2.15}$$

The superscript c denotes the correct value. The corrected accelerations are calculated from the interatomic force by using the predicted positions. The corrected accelerations can be written as

$$\ddot{r}^c(t+\delta t) = -\frac{1}{m}\vec{\nabla}\phi(r^p(t+\delta t)) \ . \tag{2.16}$$

Thus Eq. (2.15) can be regarded as a correction to the prediction step. The corrected position, velocity and acceleration can be obtain from Eq. (2.14)

and Eq. (2.15) as

$$\begin{pmatrix} r^c(t+\delta t) \\ \dot{r}^c(t+\delta t) \\ \ddot{r}^c(t+\delta t) \\ \dddot{r}^c(t+\delta t) \end{pmatrix} = \begin{pmatrix} r^p(t+\delta t) \\ \dot{r}^p(t+\delta t) \\ \ddot{r}^p(t+\delta t) \\ \dddot{r}^p(t+\delta t) \end{pmatrix} + \begin{pmatrix} C_0(\delta t)^2 \\ C_1\delta t \\ C_2 \\ C_3/\delta t \end{pmatrix} \Delta\ddot{r}(t+\delta t) \ , \qquad (2.17)$$

where C is a constant vector. The choice of C is depended on the order of the method and resulted in stability properties [44]. Gear [4] derived the constant vector $C = (\frac{1}{6}, \frac{5}{6}, 1, \frac{1}{3})$ in the fourth-order scheme by considering the optimum stability and accuracy of the solutions. As time increases, we repeat Eq. (2.14) and Eq. (2.17) for the integration.

Choice of time step

The choice of time step (δt) is an important part. If δt is too large then the system is unstable, i.e., the energy of the system is not conserved. Moreover, the truncation error which comes from the integration algorithm is dominant. In contrast, if δt is too small, the simulation time will take unnecessarily long computing time. In the simulation of solid states, δt is suggested to be much shorter than the period of typical phonons, for example Debye frequency of zirconium has period of 26 fs. Ackland [15] discussed the stability of the predictor-corrector algorithm with various δt for zirconium. He found that δt should be smaller than 5 fs. In the present work, we use 1 fs time step.

Chapter 3

Entropy in Zirconium

In this chapter, we describe the phase transition in zirconium by using the Helmholtz free energy. The bcc-hcp phase transition is one of the most frequently observation in condensed matter physics. Zirconium is an example. The structural phase transition in zirconium is martensitic meaning that it is solid to solid phase transition and requires little distortion from the parent lattice. The excessive entropy is responsible for the phase transition. In this work, we calculate the entropy of zirconium which comprises vibrational entropy and the electronic entropy. We discuss the vibrational entropy in section (3.1) and the electronic entropy in section (3.2). We also discuss briefly the electronic density of states which are calculated from the full potential linear muffin-tin orbital method (FP-LMTO) for completion.

3.1 Vibrational Entropy

The vibrational entropy, which is the entropy from the vibration of atoms in solids, comprises the harmonic vibrational entropy and the anharmonic vibrational entropy.

The historical study of the quantum description of harmonicity began since Einstein in 1907. He assumed that atoms in a crystal can be treated as independent oscillators about fixed lattice sites. Each oscillator vibrates with the same frequency $\left(\nu = \frac{\omega}{2\pi}\right)$ where ω is a typical circular frequency. In 1912, Debye suggested a more realistic model. In Debye model, the atoms no longer vibrate independently about fixed lattice sites. The dependence between normal modes is embedded in the phonon density of states. The phonon density of states is proportional to the square of the phonon frequencies. The phonon frequencies in Debye model are not higher than a maximum frequency, called ‘‘Debye frequency”. A main aim of this research is to improve Debye model. The phonon density of states is evaluated from the MD simulations. It is then a complicated function of the phonon frequencies as it implicitly includes mode-mode interactions.

In a crystalline solid, the effective interactions between atoms are cohesive energy. In the harmonic regime, the interactions are analogous to a system in which each atom contacts with springs in the x, y and z directions as shown in

Fig. (3.1).

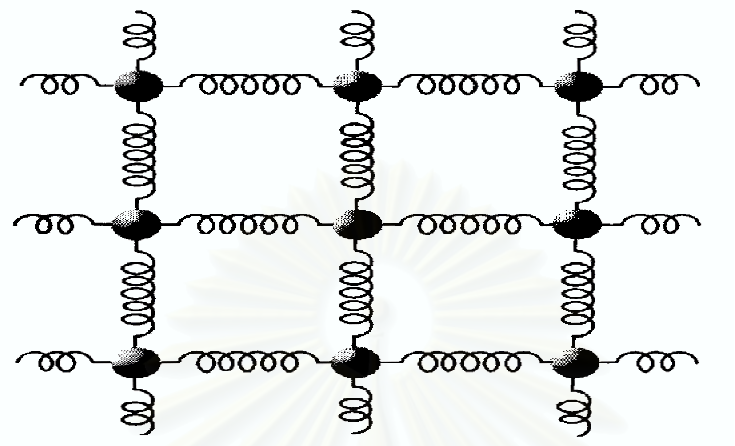

Fig. (3.1) Interactions of atoms in the harmonic regime in a planar cross-section [10].

Then each mass-spring system is corresponding with a harmonic oscillator. The Hamiltonian for a harmonic oscillator in the x-direction is

$$\widehat{H}_x = \frac{\hat{p}_x^2}{2m} + \frac{m\omega^2\hat{x}^2}{2} \ .$$

From the fundamental of quantum mechanics, we can find the energy eigenvalue of the harmonic oscillator in state n, which is

$$E_n = \hbar\omega\left(n + \frac{1}{2}\right) \ , \tag{3.1}$$

where $\hbar$ is Planck constant, n runs from 0 to ∞. Statistical mechanics is applied to calculate the harmonic vibrational entropy via the partition function (Z). We also use the partition function to calculate some other thermodynamics

parameters as they are directly connected. We are particularly interested in some thermodynamics parameters such as pressure (P), volume (V), entropy (S) and so on. The partition function per oscillator (Z_n) is defined by

$$Z_n = \sum_{\{states\}} e^{-\beta E_n} \ , \tag{3.2}$$

where E_n is energy of the oscillator in the quantum state n. $\{states\}$ is a set of all possible harmonic quantum states. $\beta = \frac{1}{k_B T}$, k_B is Boltzmann constant, T is the temperature of the system. By substituting the energy eigenvalue of the harmonic oscillators into Eq. (3.2), we get

$$\begin{aligned} Z_n &= \sum_{n=0}^{\infty} e^{-\beta\left[\hbar\omega\left(n+\frac{1}{2}\right)\right]} \ , \\ &= e^{\frac{-\beta\hbar\omega}{2}} \sum_{n=0}^{\infty} \left(e^{-\beta\hbar\omega}\right)^n \ . \end{aligned} \tag{3.3}$$

By using the geometrical series

$$\frac{1}{1-t} = \sum_{t=0}^{\infty} t^n \qquad ; |t| < 1 \ .$$

then Eq. (3.3) can be written in a fractional form as

$$Z_n = \frac{e^{\frac{-\beta\hbar\omega}{2}}}{1 - e^{-\beta\hbar\omega}} \ . \tag{3.4}$$

Next, we need to find Helmholtz free energy per oscillator (F_n) which is defined as

$$F_n = -\frac{1}{\beta} \ln Z_n \ . \tag{3.5}$$

Substitute Eq. (3.4) into Eq. (3.5), we get

$$F_n = -\frac{1}{\beta}\ln\left[\frac{e^{\frac{-\beta\hbar\omega}{2}}}{1-e^{-\beta\hbar\omega}}\right] ,$$

$$= \frac{1}{\beta}\left[\frac{\beta\hbar\omega}{2} + \ln\left(1-e^{-\beta\hbar\omega}\right)\right] ,$$

$$= \frac{\hbar\omega}{2} + \frac{1}{\beta}\ln\left(1-e^{-\beta\hbar\omega}\right) . \tag{3.6}$$

By using the relation $S = -\left(\frac{\partial F}{\partial T}\right)_V$, V is the volume of the system, S is the entropy corresponding with Helmholtz free energy (F). The harmonic vibrational entropy per oscillator is

$$S_n = -\left(\frac{\partial F_n}{\partial \beta}\right)_V \left(\frac{\partial \beta}{\partial T}\right)_V .$$

From Eq. (3.6), we find that

$$\frac{\partial F_n}{\partial \beta} = \frac{1}{\beta}\left[\frac{\hbar\omega}{e^{\beta\hbar\omega}-1} - \frac{\ln\left(1-e^{-\beta\hbar\omega}\right)}{\beta}\right] ,$$

and

$$\frac{\partial \beta}{\partial T} = -\frac{\beta}{T} .$$

Then

$$S_n = \frac{1}{T}\left[\frac{\hbar\omega}{e^{\beta\hbar\omega}-1} - \frac{\ln\left(1-e^{-\beta\hbar\omega}\right)}{\beta}\right], \tag{3.7}$$

If we define

$$P(\omega) = \frac{1}{e^{\beta\hbar\omega}-1} ,$$

$$Q(\omega) = 1 + P(\omega) ,$$

we can see some physical interpretations. Obviously, $P(\omega)$ is Bose-Einstein distribution. This is because the vibration of atoms on the lattice sites is corresponding with a phonon particle, which is of course a boson. Then Eq. (3.7) can be written in an exact form as

$$S_n = -k_B \left[P(\omega) \ln P(\omega) - Q(\omega) \ln Q(\omega) \right] \ , \tag{3.8}$$

This is the harmonic vibrational entropy per oscillator. In a real crystalline solid, if our system contains N atoms, it must have $3N$ harmonic oscillators. If we assumed that there is no interaction between each oscillator then the harmonic vibrational entropy of the system (S) is

$$S = \sum_{n=1}^{3N} S_n \ . \tag{3.9}$$

Now we introduce the phonon density of states. The phonon density of states is the number of phonons or oscillators with frequencies between ω and $\omega + d\omega$. If $d\omega$ is very small, we can change the discrete form into a continuous form as

$$\sum_{n=1}^{3N} S_n \longrightarrow \int_0^{\omega_{max}} AD(\omega) S_n \, d\omega \ ,$$

where A is a normalization constant. Then Eq. (3.9) can be written as

$$S = -k_B \int_0^{\omega_{max}} AD(\omega) \left[P(\omega) \ln P(\omega) - Q(\omega) \ln Q(\omega) \right] \, d\omega \ . \tag{3.10}$$

The phonon density of states must be normalized because we have a limit number of oscillators. Thus the phonon density of states must satisfy

$$\int_0^{\omega_{max}} AD(\omega)\, d\omega = 3N \ .$$

Then, we can solve for the normalization constant (A) which is

$$A = \frac{3N}{\int_0^{\omega_{max}} D(\omega)\, d\omega} \ .$$

Substitute the normalization constant A into Eq. (3.10), we get

$$S = \frac{-3Nk_B}{\int_0^{\omega_{max}} D(\omega)\, d\omega} \int_0^{\omega_{max}} D(\omega) \left[P(\omega) \ln P(\omega) - Q(\omega) \ln Q(\omega)\right]\, d\omega \ .$$

If we define the harmonic vibrational entropy per atom $S_{har} = \frac{S}{N}$, then

$$S_{har} = \frac{-3k_B}{\int_0^{\omega_{max}} D(\omega)\, d\omega} \int_0^{\omega_{max}} D(\omega) \left[P(\omega) \ln P(\omega) - Q(\omega) \ln Q(\omega)\right]\, d\omega \ . \quad (3.11)$$

The phonon density of states can be calculated from the velocity autocorrelation function [25]. The velocity autocorrelation function, $\gamma(t)$, which is obtained directly from the MD simulations is defined by

$$\gamma(t) = \sum_i \left[\frac{< \vec{v}_i(t) \cdot \vec{v}_i(0) >}{< v_i^2(0) >}\right] \ . \quad (3.12)$$

The average of the correlation function of the velocity [57] can be written in the discrete form as

$$\langle \vec{v}_i(t) \cdot \vec{v}_i(0) \rangle \cong \frac{1}{t_{max}} \sum_{t_0=0}^{t_{max}} \vec{v}_i(t + t_0) \cdot \vec{v}_i(t_0) \ . \quad (3.13)$$

As a consequence, the velocity autocorrelation function can be written as

$$\gamma(t) = \sum_i \left(\frac{\sum_{t_0=0}^{t_{max}} \vec{v}_i(t+t_0) \cdot \vec{v}_i(t_0)}{\sum_{t_0=0}^{t_{max}} v_i^2(t_0)} \right) . \tag{3.14}$$

We assume that each oscillator vibrates in a pure harmonic mode. The velocity of each oscillator, which has amplitude A, frequency ω and initial phase ϕ, is

$$v_i(t+t_0) = -\omega_i A_i \sin[\omega_i(t+t_0)+\phi] \ , \tag{3.15}$$

$$v_i(t_0) = -\omega_i A_i \sin(\omega_i t_0 + \phi) \ . \tag{3.16}$$

We substitute Eq. (3.15) and Eq. (3.16) into Eq. (3.14)

$$\begin{aligned} \gamma(t) &= \sum_i \left[\frac{\sum_{t_0=0}^{t_{max}} \omega_i^2 A_i^2 \sin[\omega_i(t+t_0)+\phi] \sin(\omega_i t_0 + \phi)}{\sum_{t_0=0}^{t_{max}} \omega_i^2 A_i^2 \sin^2(\omega_i t_0 + \phi)} \right] , \\ &= \sum_i \left[\frac{\sum_{t_0=0}^{t_{max}} \sin[\omega_i(t+t_0)+\phi] \sin(\omega_i t_0 + \phi)}{\sum_{t_0=0}^{t_{max}} \sin^2(\omega_i t_0 + \phi)} \right] . \end{aligned} \tag{3.17}$$

We change summation over t_0 of Eq. (3.17) into the integral form as

$$\gamma(t) = \sum_i \left[\frac{\int_0^{t_{max}} \sin[\omega_i(t+t_0)+\phi] \sin(\omega_i t_0 + \phi)\, dt_0}{\int_0^{t_{max}} \sin^2(\omega_i t_0 + \phi)\, dt_0} \right] , \tag{3.18}$$

The integral in Eq. (3.18) can be evaluated as

$$\begin{aligned} \int_0^{t_{max}} \sin[\omega(t+t_0)+\phi] \sin(\omega t_0 + \phi)\, dt_0 &= \frac{1}{2} \Bigg[\int_0^{t_{max}} \cos(\omega t)\, dt_0 \\ &\quad - \int_0^{t_{max}} \cos\left[\omega(t+2t_0)+2\phi\right]\, dt_0 \Bigg] , \end{aligned}$$

$$\int_0^{t_{max}} \sin[\omega(t+t_0)+\phi]\sin(\omega t_0+\phi)\,dt_0 = \frac{1}{2}\Bigg[t_{max}\cos(\omega t) - \frac{\sin(\omega t_{max})\cos[\omega(t+t_{max})+2\phi]}{\omega}\Bigg] , \quad (3.19)$$

By setting t=0, Eq.(3.19) is reduced to

$$\int_0^{t_{max}} \sin^2(\omega t_0+\phi)\,dt_0 = \frac{1}{2}\left[t_{max} - \frac{\sin(\omega t_{max})\cos(\omega t_{max}+2\phi)}{\omega}\right] . \quad (3.20)$$

Substitute Eqs. (3.19) and (3.20) into Eq.(3.18), we get

$$\gamma(t) = \sum_i \left[\frac{\cos(\omega_i t) - \frac{\sin(\omega_i t_{max})\cos[\omega_i(t+t_{max})+2\phi])}{\omega_i t_{max}}}{1 - \frac{\sin(\omega_i t_{max})\cos(\omega_i t_{max}+2\phi)}{\omega_i t_{max}}}\right] . \quad (3.21)$$

In present work, we used $t_{max} = 51.2ps$. Einstein frequency of zirconium is between 18 - 22 THz [22]. Consequently, the $\omega_i t_{max}$ is very large. Thus Eq. (3.21) can be reduced in the form

$$\gamma(t) \approx \sum_i \cos(\omega_i t) .$$

If we change $\sum_i cos(\omega_i t) \rightarrow \int D(\omega) cos(\omega t)\,d\omega$, the velocity autocorrelation function can be written in the form

$$\gamma(t) = \int D(\omega)\cos(\omega t)\,d\omega .$$

We use inverse Fourier transform and omit a constant coefficient associated with the transform, we find that

$$D(\omega) = \int \gamma(t)\cos(\omega t)\,dt . \quad (3.22)$$

The constant is arbitrary and can be absorbed during the normalization process. In this section, we calculate the phonon density of states by using the Fourier transform of the velocity autocorrelation function as in Eq. (3.12). Then the vibrational entropy can be evaluated via Eq. (3.11). We notice that the phonon density of states from MD simulations contain some anharmonic effects. The anharmonic effects comes from the coupling between the vibration modes of each atom. The coupling of the modes is implicitly imposed in the interatomic potential. As we fit it to the properties of real zirconium, we already put the anharmonic effects in.

However, Eq. (3.11) is not true for a system at high temperature where the anharmonicity plays importance roles. In zirconium, the importance of the anharmonicity is confirmed by Ye *et al.* [3] and Heiming *et al.* [22]. Ye *et al.* [3] used the first principles total-energy calculations with a harmonic approximation to evaluate the frequency of T_1N-point phonon of the bcc zirconium. Thus the bcc phase of zirconium cannot be stabilized under the harmonic approximation. Moreover, by analyzing neutron scattering data, Heiming *et al.* found that zirconium is strongly anharmonic. At low temperature, the effects of the anharmonicity can be neglected [26]. When we increase the temperature, the anharmonicity become dominant. From the results of Ye *et al.* [3] and Heiming *et al.* [22], we conclude that the anharmonicity cannot be left out when the system

is in a state of high temperature. We calculate the effects of the anharmonicity from the anharmonic free energy [6]. The anharmonic free energy can be written as

$$\frac{F_A(T,V)}{N-1} = -k_B T \int_{T_0}^{T} \left\{ W\left(T',V\right) - \frac{3}{2} \right\} \frac{dT'}{T'} \quad , \tag{3.23}$$

where

$$W\left(T',V\right) = \frac{\left(\langle \phi\left(T',V\right)\rangle - \phi_{min}(V)\right)}{[(N-1)k_B T']} \quad .$$

By using the relation $S = -\left(\frac{\partial F}{\partial T}\right)_V$, the anharmonic vibrational entropy with constant volume can be written in the exact form as

$$\begin{aligned} \frac{S_A(V,T)}{N-1} = k_B \Bigg[& W\left(V,T\right) - \frac{T}{T_0} W\left(V,T_0\right) \\ & -\frac{3}{2}\left(1-\frac{T}{T_0}\right) + \int_{T_0}^{T} \left(W\left(V,T'\right) - \frac{3}{2} \right) \frac{dT'}{T'} \Bigg] \ , \end{aligned} \tag{3.24}$$

where $\phi_{min}(V)$ is minimum potential energy at constant volume, $\langle \phi(T,V)\rangle$ is the ensemble average of the potential energy at thermodynamics equilibrium, N is the number of atoms in the system, T_0 is low temperature where the system does not have the anharmonic effects. According to Eq. (3.24), if we set $T = T_0$, the anharmonic vibrational entropy is zero. From Eq. (3.24), we can notice that the anharmonic effects is adjuncted from the harmonic effects.

3.2 Electronic Entropy

The electronic entropy relates to the atomic configuration i.e. bcc, hcp or fcc and so on. The entropy dues to a corresponding electronic structure is called the "electronic entropy ". We can calculated the electronic entropy via the grand partition function. The grand partition function is the partition function of the grand canonical ensemble or macro canonical ensemble. In grand canonical ensemble, the system of interest can exchange both energies and particles with the environment. In this situation, the atoms in a solid are arranged on the lattice sites with a specific structure. The atoms from the environment can be transferred inside or outside of the system of interest. However, the energy (E) and the number of particles (N) in the system of interest must satisfy

$$E = \sum_k n_k E_k \ , \tag{3.25}$$

$$N = \sum_k n_k \ . \tag{3.26}$$

n_k, which is called the "occupation number of state k", is the number of particles in a given single particle state k. For a fermion particle, n_k is only 0 or 1 because of Pauli-Exclusion principle. n_k= 0 is that no particle can occupy in state k. n_k=1 is that a particle can occupy in state k. If we assumed that the number of particles in the system of interest is very large, $N \to \infty$, we can define the grand

partition function (L) [5, 10, 11, 45] as

$$L(\mu, V, T) = \sum_{N=0}^{\infty} e^{\beta\mu N} Z_N(V, T) \ , \tag{3.27}$$

where $\beta = \frac{1}{k_B T}$, μ is the chemical potential which describes the mobility of particles transferred between the system of interest and the environment. μ must satisfy

$$n = \int_{-\infty}^{\infty} f(E) g(E)\, dE \ .$$

$f(E) = \left(1 + e^{\frac{E-\mu}{k_B T}}\right)^{-1}$ is Fermi-Dirac distribution. $g(E)$ is the electronic density of states. n is the number of electrons in the conduction band. $Z_N(V, T)$ is the canonical partition function which is defined by

$$Z_N(V, T) = \sum_{\{n_i\}} e^{-\beta E(n_i)} \ , \tag{3.28}$$

where the set of occupation numbers must satisfy Eq. (3.26). When we substitute Eq. (3.25), Eq. (3.26) and Eq. (3.28) into Eq. (3.27), we get

$$L(\mu, V, T) = \sum_{N=0}^{\infty} \sum_{\{n_k\}} e^{\beta\mu \sum_k n_k} e^{-\beta \sum_k n_k E_k} \ , \tag{3.29}$$

$$= \sum_{N=0}^{\infty} \sum_{\substack{n_1, n_2, \ldots \\ \{\sum_k n_k = N\}}} e^{\beta\mu(n_1 + n_2 + \ldots)} e^{-\beta(n_1 E_1 + n_2 E_2 + \ldots)} \ ,$$

$$= \sum_{N=0}^{\infty} \sum_{\substack{n_1, n_2, \ldots \\ \{\sum_k n_k = N\}}} e^{\beta n_1(\mu - E_1)} e^{\beta n_2(\mu - E_2)} \ldots \ ,$$

$$= \sum_{N=0}^{\infty} \sum_{\substack{n_1,n_2,... \\ \{\sum_k n_k = N\}}} \prod_k e^{\beta n_k(\mu - E_k)} \ . \tag{3.30}$$

For $N \to \infty$, we can change double summation in Eq. (3.30) into sum of each occupation number n_k independently. Then we get

$$L(\mu, V, T) = \sum_{n_1} \sum_{n_2} ... \left(e^{\beta(\mu - E_1)}\right)^{n_1} \left(e^{\beta(\mu - E_2)}\right)^{n_2} ... \ ,$$

$$= \left[\sum_{n_1} \left(e^{\beta(\mu - E_1)}\right)^{n_1}\right] \left[\sum_{n_2} \left(e^{\beta(\mu - E_2)}\right)^{n_2}\right] ... \ .$$

Now we can write

$$L(\mu, V, T) = \prod_k \left[\sum_{n_k} \left(e^{\beta(\mu - E_k)}\right)^{n_k}\right] \ , \tag{3.31}$$

because the atom which composes of proton, neutron and electron is a fermion particle, the occupation number is only 0 or 1. Eq. (3.31) can be written as

$$L(\mu, V, T) = \prod_k \left[1 + e^{\beta(\mu - E_k)}\right] \ . \tag{3.32}$$

The electronic Helmholtz free energy (F_E) is

$$F_E = -\frac{1}{\beta} \ln L(\mu, V, T) \ .$$

Using $L(\mu, V, T)$ from Eq. (3.32), then

$$F_E = -\sum_k \frac{\ln\left(1 + e^{\beta(\mu - E_k)}\right)}{\beta} \ .$$

By using the relation $S_E = -\left(\frac{\partial F_E}{\partial T}\right)_V$, the electronic entropy at constant volume is

$$S_E = -\left(\frac{\partial F_E}{\partial \beta}\right)_V \left(\frac{\partial \beta}{\partial T}\right)_V \ ,$$

where

$$\frac{\partial F_E}{\partial \beta} = \sum_k \frac{E_k - \mu}{\beta}\left[\frac{1}{1+e^{\beta(E_k-\mu)}}\right] + \frac{\ln(1+e^{\beta(\mu-E_k)})}{\beta^2} \ ,$$

$$\frac{\partial \beta}{\partial T} = -\frac{\beta}{T} \ .$$

Consequently, the electronic entropy can be written as

$$S_E = \sum_k \frac{E_k - \mu}{T}\left[\frac{1}{1+e^{\beta(E_k-\mu)}}\right] + \frac{\ln(1+e^{\beta(\mu-E_k)})}{\beta T} \ .$$

If we define the fermi-dirac distribution, $f(E)$, which is

$$f(E) = \frac{1}{1+e^{\beta(E-\mu)}} \ ,$$

we can verify that

$$\frac{E_k - \mu}{T} = k_B \ln\left[\frac{1-f(E_k)}{f(E_k)}\right] \ ,$$

$$1 + e^{\beta(\mu-E_k)} = \frac{1}{1-f(E_k)} \ .$$

We find that

$$S_E = \sum_k k_B f(E_k) \ln\left[\frac{1-f(E_k)}{f(E_k)}\right] + k_B \ln\left[\frac{1}{1-f(E_k)}\right] \ .$$

The electronic entropy can be written in term of fermi-dirac distribution function as

$$S_E = -k_B \sum_k [1 - f(E_k)] \ln[1 - f(E_k)] + f(E_k) \ln f(E_k) \ . \tag{3.33}$$

We change the summation over each state k into the integral of the electronic density of states form. The physical meaning of the electronic density of states is same as the phonon density of states. Hence we can write the electronic entropy in the exact form as

$$S_E = -k_B \int g(E) \left[(1 - f(E)) \ln(1 - f(E)) + f(E) \ln f(E) \right] dE \ . \tag{3.34}$$

From Eq. (3.34), we use non-interacting fermion particles to derive the electronic entropy (S_E). The interactions between atoms in solid are implicitly included in the electronic density of states. The calculation of electronic density of states can be obtained from the calculation of an energy band such as Tight Binding method (TB), the Augmented Plane Wave method (APW), the Orthogonalized Plane Wave method (OPW) or the Green's function of Korringa, Kohn and Rostoker method (KKR) and so on. The difference between the energy band and the electronic density of states is that the energy band is a curve of the energy of particles as a function of wave vector k in reciprocal lattice space and wave vector k whereas the electronic density of states is a curve of the number of particles at energy level E as a function of energy E. The calculation of the electronic

density of states of zirconium is taken from Eriksson *et al.* [26] and Ahuja *et al.* [37].

Chapter 4

Results and Discussion

In this chapter, we evaluate the components of the Helmholtz free energy in order to describe the bcc-hcp phase transition and calculate the transition temperature in zirconium. We employ constant volume and temperature in every simulation. At the beginning, the system is in an arbitrary state. After that the system evolves to an equilibrium state. The trend of the Helmholtz free energy is decreasing. At thermodynamics equilibrium, the Helmholtz free energy is always a minimum. That is "the system stays in the state which the Helmholtz free energy is lowest ". If we define $\Delta F = F_{bcc} - F_{hcp}$, where F_{bcc} and F_{hcp} are Helmholtz free energy of the bcc and the hcp phases, respectively. we can write

$$\Delta F = \Delta U - T\Delta S \ . \tag{4.1}$$

If $\Delta F > 0$ or $\Delta U > T\Delta S$, Helmholtz free energy of the bcc phase higher than that of the hcp phase. As a result, the stable phase is the hcp phase. If $\Delta F < 0$ or $\Delta U < T\Delta S$, the stable phase is the bcc phase. The temperature,

where gives the condition $\Delta F = 0$ or $\Delta U = T\Delta S$, is called the "transition temperature".

In the present work, we use 8192 atoms for the bcc and 6912 atoms for the hcp phases. The temperature used in our simulations is varied from 300 to 1800 K. Next, we calculate the components of the Helmholtz free energy such as the internal energy difference between the bcc and the hcp phases (ΔU) and the entropy difference of both phases (ΔS). The results of the internal energy and the entropy of both phases are shown in section (4.1) and section (4.2) respectively.

4.1 Internal energy

The objective of this section is to calculate the internal energy difference (ΔU). The internal energy is composed of the kinetic energy (E_k) and the potential energy (ϕ). We calculate the potential energy by classical Molecular dynamics method. This method produces the time evolution of the system. At the beginning, the system is in a non-equilibrium state. After a few picosecond, the system approaches to the thermodynamics equilibrium. We average the potential energy which is Eq. (2.2) during the equilibrium. Notice that we calculate the potential energy only because the average kinetic energy at the equilibrium depends only on temperature. From equipartition theorem [29], the average kinetic energy per atom is $\frac{3}{2}k_BT$. When the temperature of both phases are equal, the kinetic

energy of both phases are cancelled out. Therefore, $\Delta U = \Delta\phi$. Moreover, by setting constant volume for all simulations, the results from the simulation of both phases excludes thermal expansion effects. The calculation of the potential energy due to the thermal expansion can be used to classify the system into two types which is the a first system and a second system. The schematic of the first system and the second system are shown in Fig. (4.1).

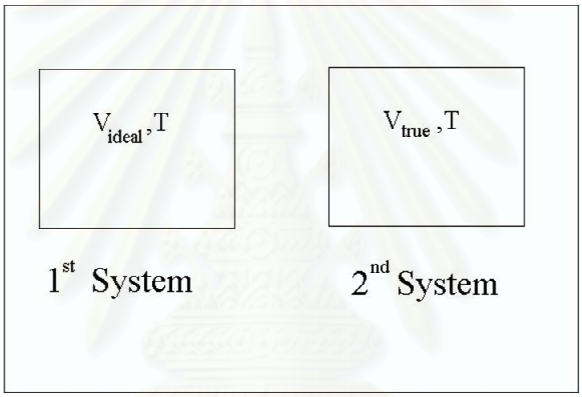

Fig. (4.1) The schematic of 1^{st} and 2^{nd} systems for computing the potential energy and the entropy from the thermal expansion, where V_{ideal} is the volume corresponding with T=0 K and V_{true} is the volume corresponding with $P = 0$.

The first system has an ideal volume (V_{ideal}) in which zirconium is at absolute zero temperature. The second system has a true volume (V_{true}), which is corresponding with zero pressure. The physical meaning of $P = 0$ is that there is no external work acting on the simulation box. Then the total work acting on the simulation box is equal to the internal work. According to Eq.

(2.9), the simulation box will receive the energy, which comes from the total work, until it has temperature T. Then the volume of the simulation box is changed by the total work that acting on the simulation box. From Eq. (2.10), the change in the volume in response to the total work is equal to the change in the volume in response to the internal work or interatomic interactions. So the volume corresponding with $P = 0$ is a true volume, which includes the thermal expansion effects. The true volume of the bcc and hcp phases are shown in term of the lattice constant values as in Fig. (4.2) and Fig. (4.3) respectively.

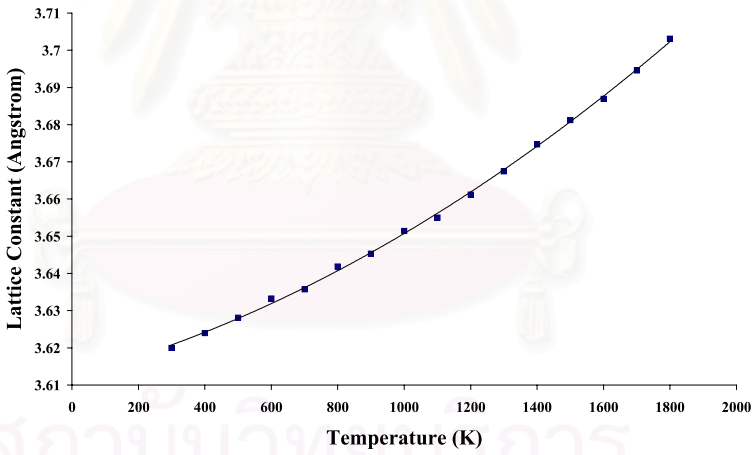

Fig. (4.2) The true lattice constant corresponding with the P=0 in the bcc phase.

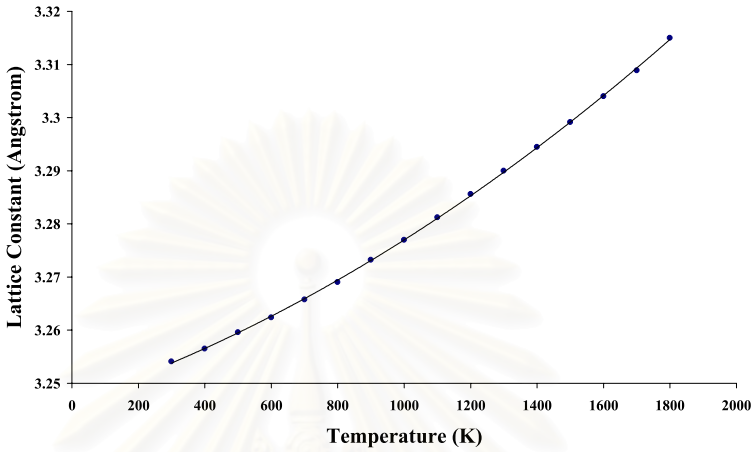

Fig. (4.3) The true lattice constant corresponding with the P=0 in the hcp phase.

We define the potential energy from the first and the second systems which are $\phi\left(V_{ideal}, T\right), \phi\left(V_{true}, T\right)$ respectively. The difference between the first and the second systems are in their volumes. The potential energy difference between the first and the second systems are the potential energy from the expansion of the volume or the potential energy from the thermal expansion ($\phi_{thermal}$). That is

$$\phi_{thermal} = \phi\left(V_{true}, T\right) - \phi\left(V_{ideal}, T\right) \ . \tag{4.2}$$

The potential energy of the system can be written as

$$\phi = \phi\left(V_{ideal}, T\right) + \phi_{thermal} \equiv \phi\left(V_{true}, T\right) \ . \tag{4.3}$$

The potential energy of the bcc and the hcp phases at true volume are shown in Fig. (4.4). At the same temperature, the difference between potential energy of the bcc and hcp phases is ΔU.

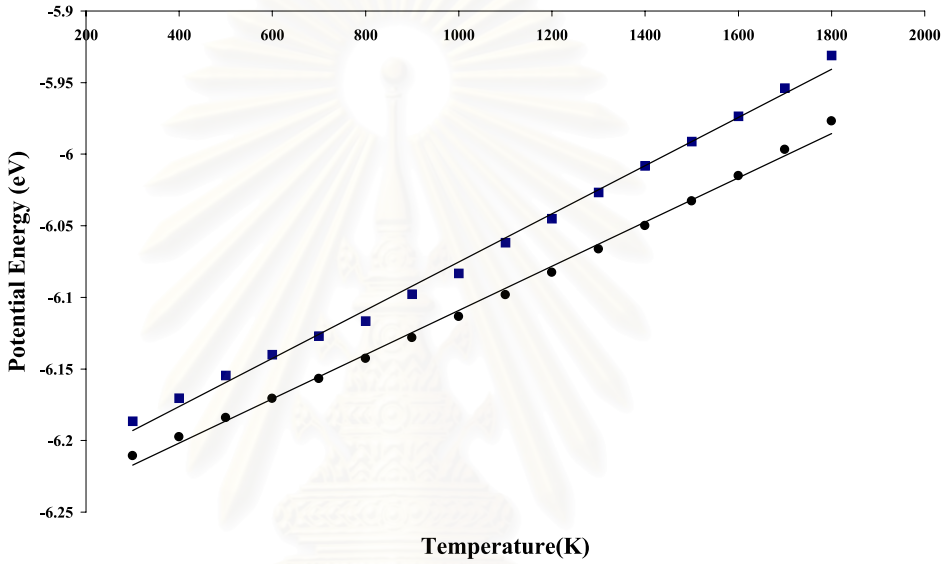

Fig. (4.4) The averaged potential energy of the bcc (squares) and the hcp (circles) phases as a function of temperature from MD simulations.

4.2 Entropy

The entropy can be separated into two parts, the vibrational entropy (S_{vib}) and the electronic entropy (S_E). The results of the vibrational entropy and the electronic entropy are shown in section (4.2.1) and section (4.2.2) respectively.

4.2.1 Vibrational Entropy

The vibrational entropy comprises the harmonic vibrational entropy and the anharmonic vibrational entropy. The harmonic vibrational entropy can be calculated via Eq. (3.11) which is depended on the phonon density of states (DOS). The DOS is determined from the velocity autocorrelation function (VACF) that is defined in Eq. (3.12). We apply power spectrum method to the VACF and get the DOS as proved in Eq. (3.22). We have done the calculations between T = 300 and 1800 K. We choose the power spectrum method to calculate the DOS because the results from this method have only positive values which are in an agreement with the definition of the DOS. The VACF and the DOS at T=1300 K for bcc and hcp phases are shown in Figs. (4.5-4.8) as a sample of typical VACF and DOS functions.

Next, we use the DOS to calculate the harmonic vibrational entropy via Eq. (3.11). We get the harmonic vibrational entropy as a function of temperature. The harmonic vibrational entropy of the bcc and hcp phases are shown in Fig. (4.9) and Fig. (4.10) respectively.

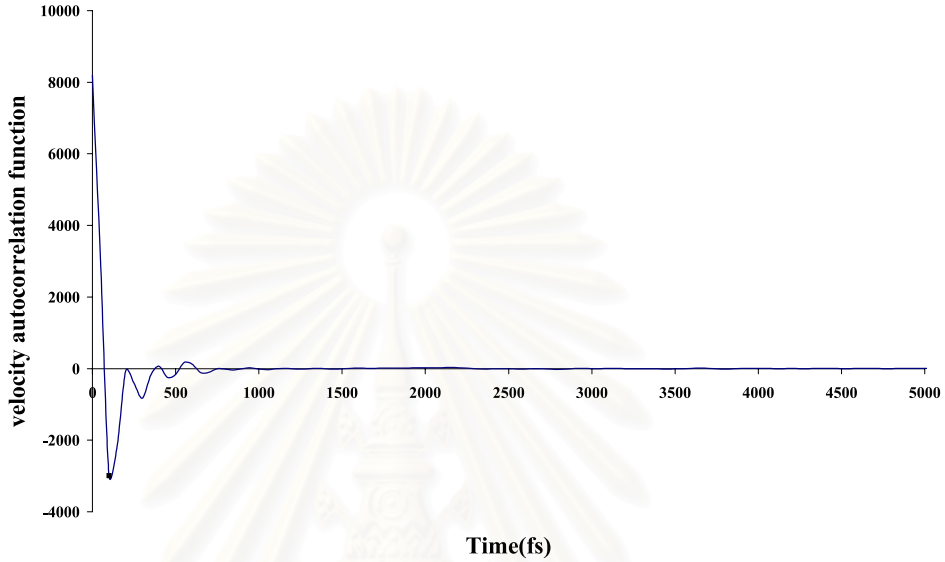

Fig. (4.5) The velocity autocorrelation function from MD simulations with 8192 atoms for the bcc phase at T = 1300 K.

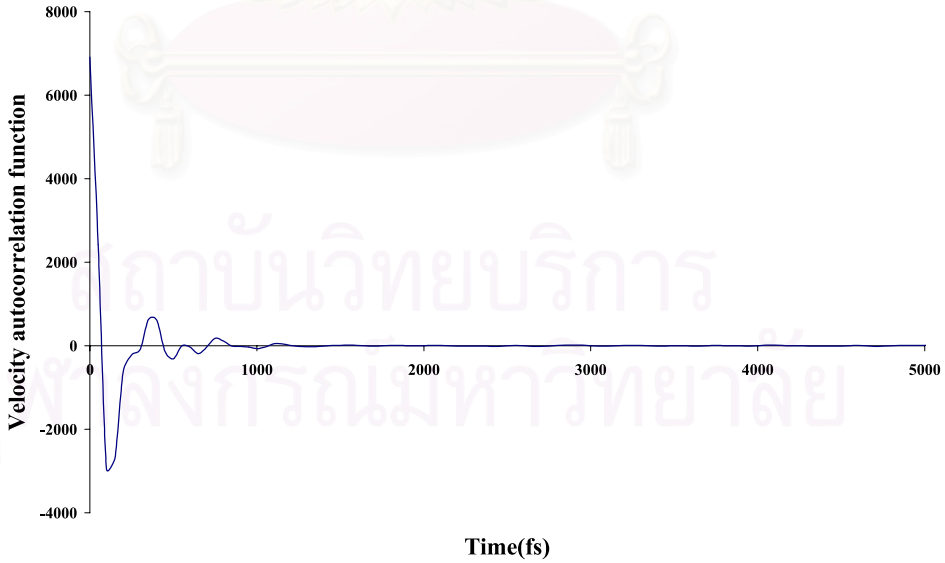

Fig. (4.6) The velocity autocorrelation function from MD simulations with 6912 atoms for the hcp phase at T = 1300 K.

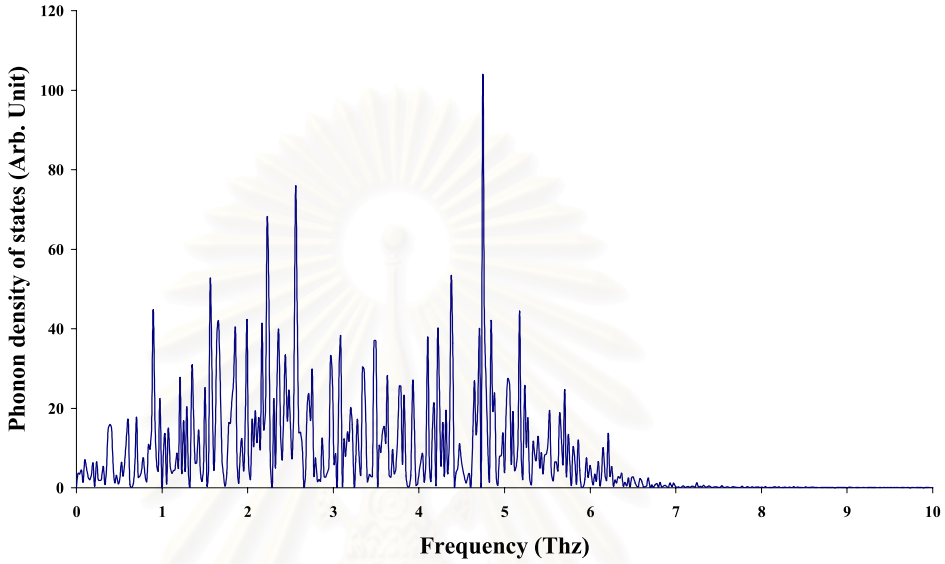

Fig. (4.7) The phonon density of states of the bcc phase at T=1300K.

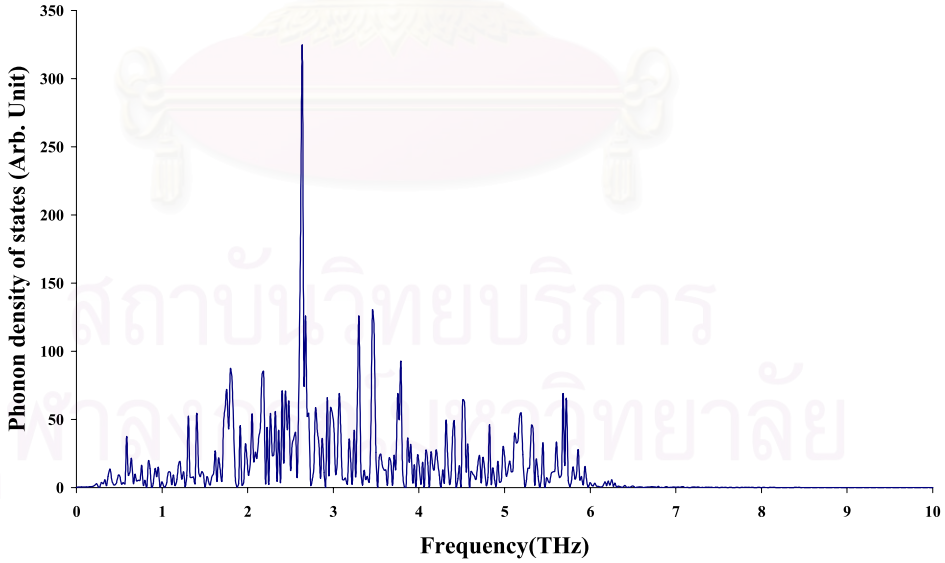

Fig. (4.8) The phonon density of states of the hcp phase at T=1300K.

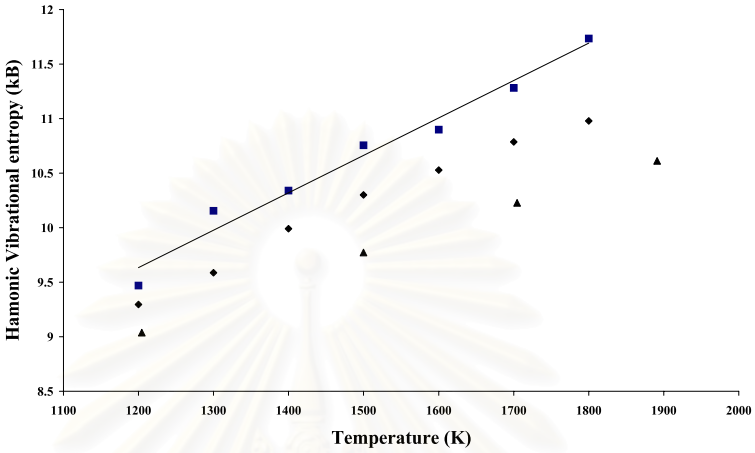

Fig.(4.9) The harmonic vibrational entropy in the bcc phase (squares), compared with the results from the Einstein crystal method (triangles) [9] and the results calculated with the ideal volume (diamonds) [38]. The solid line is a linear least squares fit.

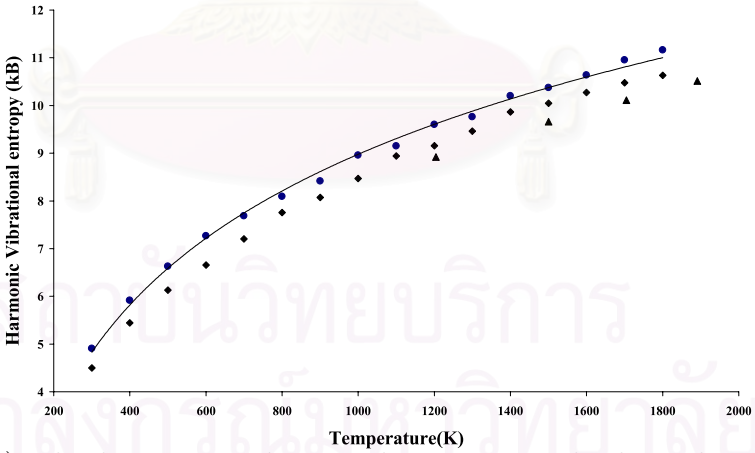

Fig.(4.10) The harmonic vibrational entropy in the hcp phase (circles), compared with the results from the Einstein crystal method (triangles) [9] and the results calculated with the ideal volume (diamonds) [38] . The solid line is a logarithmic least squares fit.

In our simulations, the harmonic vibrational entropy of the bcc phase at the temperature lower than or around the transition temperature cannot be evaluated because the system undergoes a phase transition from the bcc to the hcp phase. However, the system has been in the bcc phase for a short period. This period is long enough so that we can determine the average potential energy of the bcc phase but we can not calculated the DOS because this period is too short to obtain statistically reliable results. Thus the calculation of the DOS at this temperature is not accurate and we do not use it.

We notice that the harmonic vibrational entropy with the true volume, $S(V_{true}, T)$, contains some anharmonic effects. It contains the coupling between the vibration modes which are encapsulated in the phonon density of states from the MD simulations. Moreover, it contains the thermal expansion effects because we change the volume of the system until the pressure of the system is zero whereas the results from the Einstein crystal method do not included the coupling between the vibration modes.

However, the calculation of the harmonic vibrational entropy is not an exact vibrational entropy because the anharmonic effects plays an important role at high temperature. The anharmonic effects cause thermal resistivity and the difference between constant pressure and constant volume specific heat in the lattice. Thus we must add the anharmonic vibrational entropy which can be cal-

culated using Eq. (3.24). The ideal volume is chosen to calculate the anharmonic vibrational entropy because the effects of the expansion of the volume are already included in the harmonic calculations. The anharmonic vibrational entropy of the bcc and hcp phases are shown in Fig. (4.11).

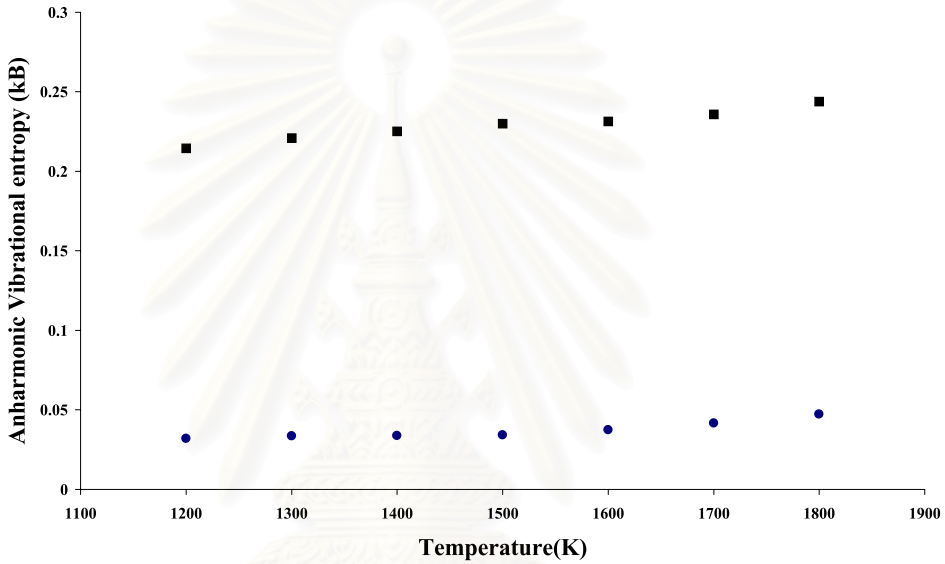

Fig. (4.11) The anharmonic vibrational entropy of the bcc (squares) and the hcp (circles) phases as a function of temperature.

The calculation of the entropy from thermal expansion is the same as the calculation of the potential energy from the thermal expansion. According to Fig. (4.3), if we define the entropy from the first and the second systems which are $S(V_{true}, T)$ and $S(V_{ideal}, T)$ respectively. $S(V_{ideal}, T)$ (diamond points) is shown in Fig. (4.9) and Fig. (4.10). Eq. (3.11) is used in order to evaluate the entropy. The entropy difference between the first and the second systems is the

result of the expansion of the volume or the entropy due to the thermal expansion ($S_{thermal}$). Thus the entropy from the thermal expansion can be written as

$$S_{thermal} = S_{har}(V_{true}, T) - S_{har}(V_{ideal}, T) \ . \tag{4.4}$$

In experiments, we cannot measure the pure harmonic vibrational entropy. The results from neutron scattering experiments contain the harmonic, the anharmonic and the thermal expansion effects. Hence we must calculate all contributions to the vibrational entropy in order to compare the results from our simulation with the experimental results. The vibrational entropy can be written as

$$S_{vib} = S_{har}(V_{ideal}, T) + S_A(V_{ideal}, T) + S_{thermal} \ . \tag{4.5}$$

The vibrational entropy of the bcc and hcp phases are shown in Fig. (4.12) and Fig. (4.13) respectively.

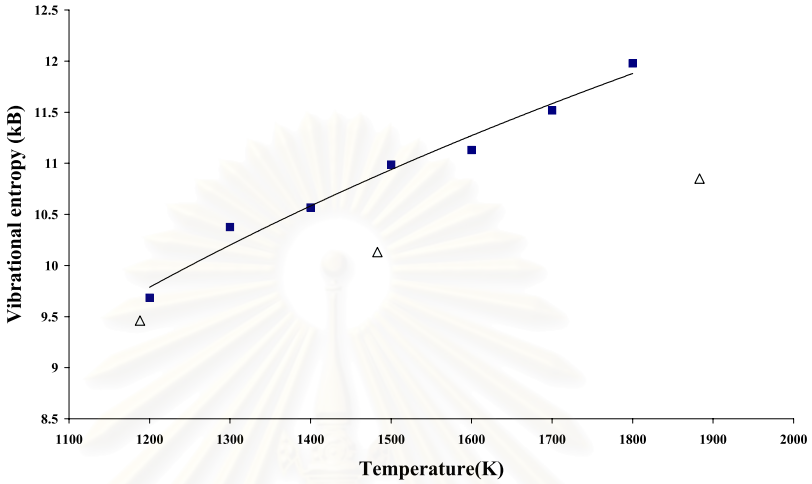

Fig. (4.12) The vibrational entropy of the bcc phase (squares) compared with the experimental results (open triangles) [22]. The solid line is a linear least square fit.

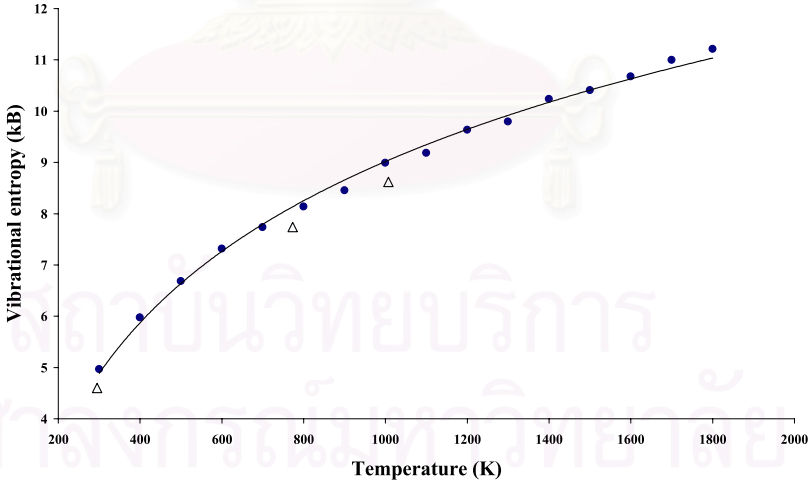

Fig. (4.13) The vibrational entropy of the hcp phase (circles) compared with the experimental results (open triangles) [22]. The solid line is a logarithmic least square fit.

From Fig. (4.12) and Fig. (4.13), we apply a logarithmic extrapolation in the vibrational entropy in the hcp phase and a linear extrapolation in the vibrational entropy in the bcc phase. We find that the vibrational entropy difference between the bcc and hcp phases, ΔS_{vib}, at 1135 K is 0.20 k_B compared with 0.12-0.14 k_B from the results of Willaime [12] and Salomon [9]. ΔS_{vib} from experimental results is 0.26 k_B [19, 22].

4.2.2 Electronic Entropy

The electronic entropy can be calculated by using the electronic structure of materials. The electronic entropy is calculated via Eq. (3.34). In this work, we used non-interacting fermion model to calculate the electronic entropy. The interaction of each fermion particle already implicitly includes in the electronic density of states. We use the electronic density of states which is obtained from Ahuja *et al.* [37]. The electronic density of states are evaluated from the full potential linear muffin tin orbital method (FP-LMTO) [20, 21, 33, 35]. The electronic density of states of the bcc and hcp phases are shown in Figs. (4.14-4.15).

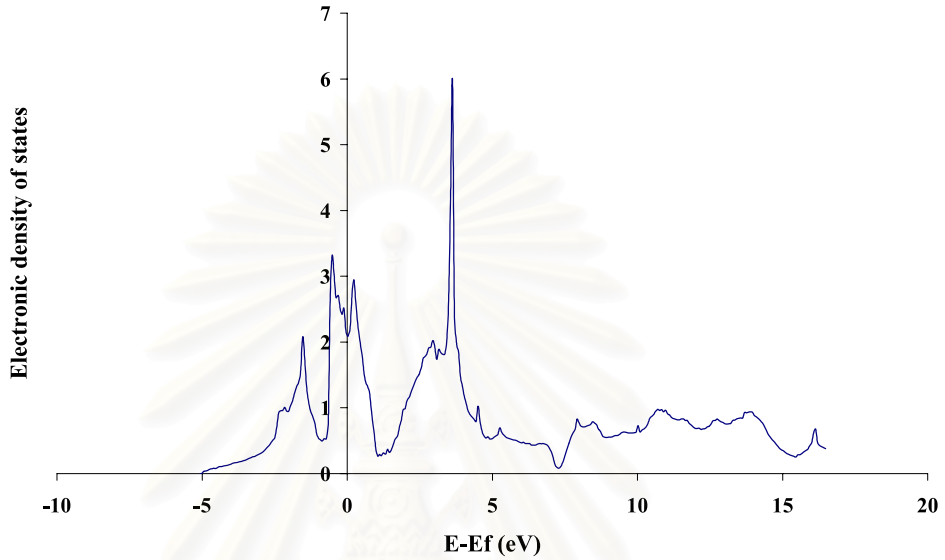

Fig. (4.14) The electronic density of states of the bcc phase at absolute zero temperature [37].

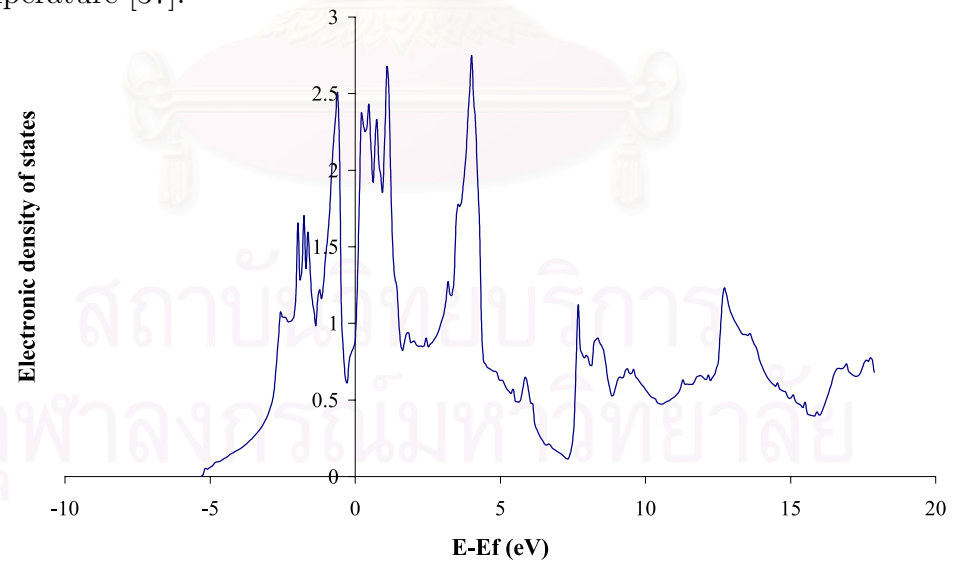

Fig. (4.15) The electronic density of states of the hcp phase at absolute zero temperature [37].

The electronic density of states at absolute zero temperature is chosen because we do not include the thermal expansion effects in the results of the electronic entropy. However, the Fermi temperature of the free electron gas in metals is about 10^5 K, which is quite high compared with temperatures in our simulation. Thus the effect of temperature to the electronic density of states can be neglected. From Eq. (3.34), we notice that the distribution of the fermion particles must agree with the Fermi-Dirac distribution. The electronic entropy as a function of temperature in the Fermi-Dirac distribution form is shown in Fig. (4.16) and Fig. (4.17) respectively.

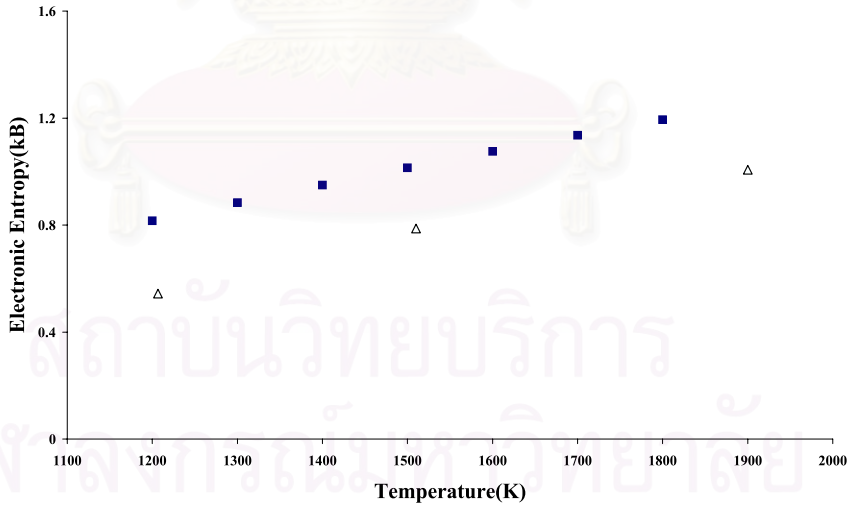

Fig. (4.16) The electronic entropy of the bcc phase (squares) compared with experimental results from Eriksson *et al.* [26] (open triangles).

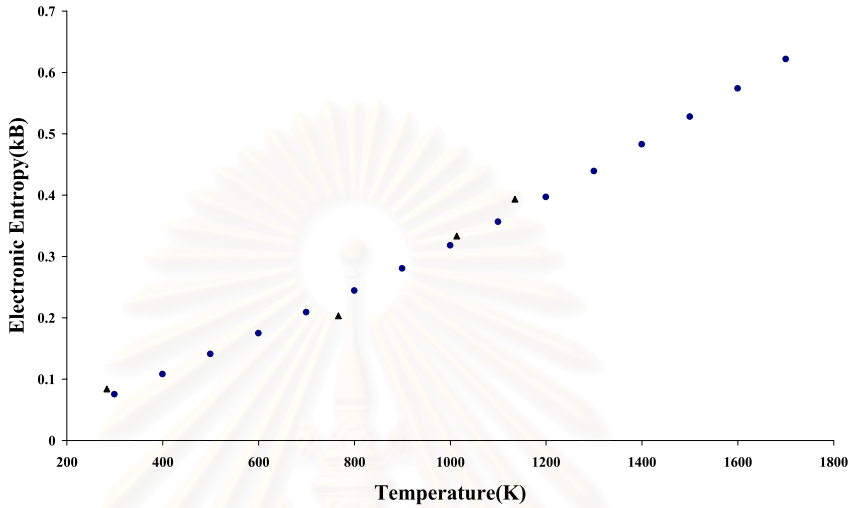

Fig. (4.17) The electronic entropy of the hcp phase (circles) compared with experimental results from Eriksson *et al.* [26] (open triangles).

Watson and Weinert [54] estimated the electronic entropy to lowest order in temperature as $\left(\frac{\pi^2}{3}\right) n\left(E_F\right) k_B^2 T$, where $n\left(E_F\right)$ is the electronic density of states at the Fermi level. From Fig. (4.14) and Fig. (4.15), the electronic density of states at the Fermi level of the bcc phase is higher than the hcp phase. Consequently, the electronic entropy of the bcc phase is higher than the hcp phase which is in agreement with our calculations results. In addition, the trends of the electronic entropy from our calculations is almost linearly in temperature which is in agreement with the estimation from Watson and Weinert [54]. Now we can

evaluate the total entropy which can be written as

$$S_{tot} = S_{vib} + S_E \ .$$

The total entropy of the bcc and the hcp phases are shown in Fig. (4.18).

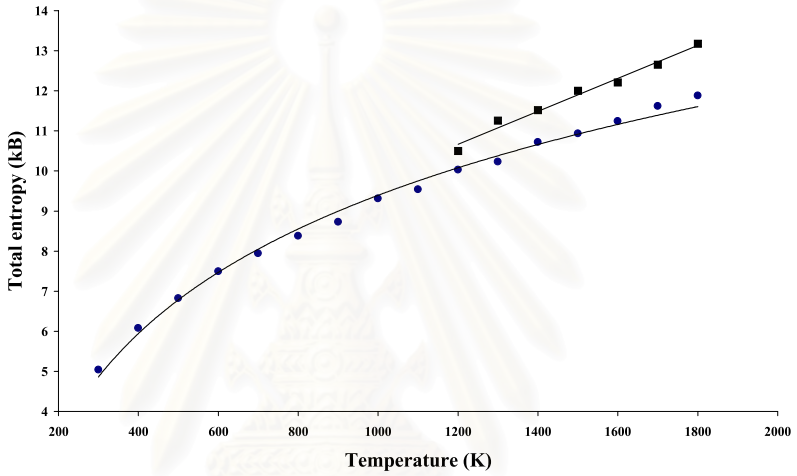

Fig. (4.18) The total entropy of the bcc (squares) and hcp phases (circles) at various temperature.

Next, we calculate ΔU which comes from Fig. (4.4) and $T\Delta S$. The result of ΔU and $T\Delta S$ are shown in Fig.(4.19).

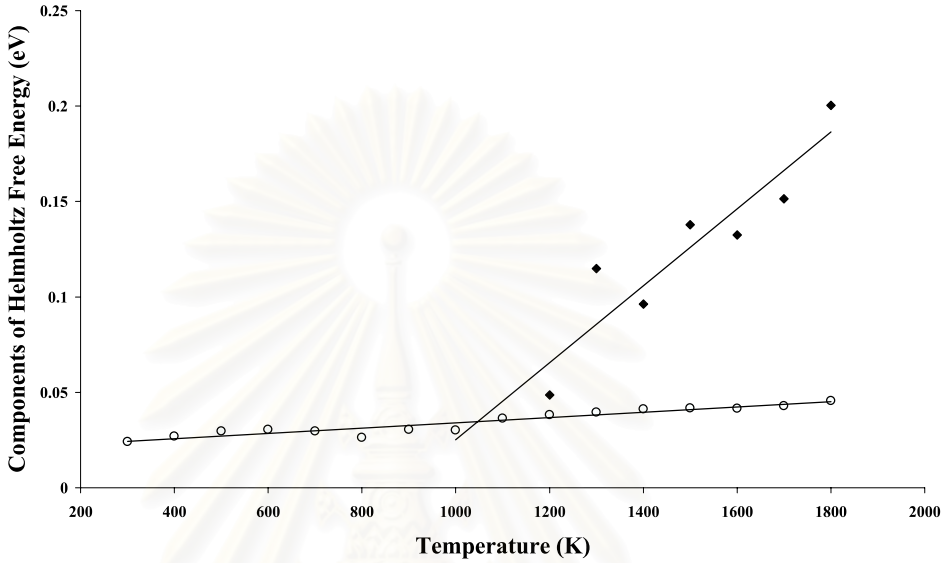

Fig. (4.19) Components of the Helmholtz free energy, i.e., ΔU (open circles) and $T\Delta S$ (diamonds).

The intersection between ΔU and $T\Delta S$ is the transition temperature. From Fig. (4.19), we find a transition temperature of 1047 $\pm$ 210 K compared with 1850 K from Salomon [9], 1912 K by Willaime and Massobrio [12], 1754 K from Pinsook [36] and 1135 K from experiments [1, 2, 22]. The disagreement of the previous theoretical transition temperature arises because they did not fully consider the effects of the anharmonicity and the electronic structure. In some transition metals including zirconium, Eriksson *et al.* [26] and Bogdanoff *et al.* [24] showed that the total entropy can be decomposed into the vibrational entropy

and the electronic entropy. This principle can be applied to other materials such as Li [7], NiAl alloys [39], Ti [19] and Fe [46] where the electrons and the phonons have no strong mutual interactions, otherwise the entropy cannot be decomposed and the results will be incorrect. Then one must apply a more sophisticated tool. However, this method is classical and the simulation results are valid when the temperature of the system is higher than Debye temperature [56]. Recently, there has been a report on a purely quantum mechanical treatment of phonon in zirconium [55]. Thus this method might be very helpful for the simulation at low temperature where the quantum effects play a dominate roles. Furthermore, if materials have magnetic effects, the entropy from magnetic effects must also be included.

Chapter 5

Conclusions

The bcc-hcp phase transition is the focus of this research. We perform the classical Molecular Dynamics method to simulate zirconium in the bcc and the hcp phases. This method can be used for studying the anharmonic effects and gives agreement with those of the perturbation method [6]. In addition, Lack [6] argues that the free energy from MD simulations were found to converge more quickly than Monte Carlo simulation. The temperature, which is used in this simulations, must higher than Debye temperature because of the validity of classical mechanics regimes. If the temperature is lower than Debye temperature, the quantum effects play dominate roles. Hence the classical mechanics is broken down. The constant volume and temperature conditions are set in each simulation. We choose the Finnis-Sinclair interatomic potential model because it is in a simple form and accurately represents zirconium. Moreover, the Gear Predictor-Corrector integration scheme is used for integrating the Newton equations of

motion.

We choose the classical Molecular Dynamics method to determine the average potential energy during thermodynamics equilibrium and the velocity autocorrelation function of zirconium in the bcc and the hcp phases at various temperature. The entropy, which comprises the vibrational entropy and the electronic entropy, is evaluated. The vibrational entropy includes the harmonic and the anharmonic parts. The harmonic vibrational entropy and the phonon density of states are calculated from the velocity autocorrelation function. The anharmonic vibrational entropy is evaluated from the anharmonic free energy [6]. The electronic entropy can be determined from the electronic density of states which comes from the full potential linear muffin tin orbital method(FP-LMTO) [20, 21, 33, 35].

By considering Helmholtz free energy, we found that the transition temperature of zirconium is 1047 $\pm$ 210 K, compared with 1912 K from Willaime and Massobrio [12], 1850 K from Salomon [9], 1754 K from Pinsook [36] and 1135 K from experiments [1, 2, 22]. Moreover, the vibrational entropy difference between both phase is 0.20 k_B at 1135 K, comparing with 0.143 k_B from Willaime and Massobrio [12], 0.126 k_B from Salomon [19] and 0.26 k_B from experiments [19, 22]. Hence our results is in a good agreement with experimental results.

Finally, we conclude that the classical Molecular Dynamics method is a

powerful tool for studying the bcc-hcp phase transition in zirconium. Moreover, it is used for studying dynamical properties of Au [30], correlations in the motions of atoms in liquid Argon [47], dynamics of biological system such as protein, DNA, RNA [48] and lipid bilayers [49], structure of amorphous aluminium silicate [51] and Cu-Ni alloys [50], point defects and stacking faults in $TiSi_2$ [52] and phase transition of hydrogen bonded type of ferroelectric [53].

Bibliography

[1] Guillermet, A.F., "Critical evaluation of the thermodynamics properties of zirconium", *High Temp-High Press.*, **19**, (1987): 119.

[2] Kaufmann, A.R. and Magel, T.T., *Metallurgy of zirconium* edited by Lustman, B. and Kerze, F., New York: McGraw-Hill, (1995).

[3] Ye, Y.-Y., Chen, Y., Ho, K.-M., Harmon, B.N., and Lindgård, P.-A., "Phonon-Phonon coupling and the stability of the high-temperature bcc phase of Zr", *Phys.Rev.Lett.*, **58**, (1987): 1769.

[4] Gear, C.W., *Numerical Initial Value Problems in Ordinary Differential Equations*, New Jersey: Prentice-Hall, (1971).

[5] Amit, D.J., and Verbin, V., *Statistical Physics: An Introductory Course.* translated form the Hebrew by Tzafriri, R., Singapore: World Scientific , (1999).

[6] Lack, D.J., and Shukla, R.C., "Molecular dynamics and higher-order perturbation-theory results for the anharmonic free energy and equation of state of a Lennard-Jones solid", *Phys.Rev.B.*, **54**, (1996): 3266.

[7] Liu, A.Y., Quong, A.A., Freericks, J.K., Nicol, E.J., and Jones, E.C., "Structural phase stability and electron-phonon coupling in lithium" , *Phys.Rev.B.*, **59**, (1999): 4028.

[8] Ercolessi, F., *A Molecular Dynamics Primer*, Triestre: Spring college in computational physics, (1997).

[9] Salomon, E., "hcp-bcc transition and the free energies of the hcp and bcc structures of zirconium", *Phys.Rev.B.*, **43**, (1991): 6167.

[10] Mandl, F., *Statistical Physics*, Great Britain: John Wiley & Sons, (1988).

[11] Reif, F., *Fundamental of statistical and thermal physics*, Singapore: McGraw-Hill, (1985).

[12] Willaime, F., and Massobrio, C., "Temperature-Induced hcp-bcc phase transformation in zirconium : A lattice and Molecular-Dynamics study based on an N-body potential" , *Phys.Rev.Lett.*, **63**, (1989): 2244.

[13] Willaime, F., and Massobrio, C., "Development of an N-body interatomic potential for hcp and bcc zirconium", *Phys.Rev.B.*, **43**, (1991): 11653.

[14] Moroni, E.G., Grimvall, G., and Jarlborg, T., "Free energy contributions to the hcp-bcc transformation in transition metals", *Phys.Rev.Lett.*, **76** , (1996): 2758.

[15] Ackland, G.J., "Non-Pairwise potentials and defect modellimg for transition metals", *Ph.D. Thesis*, Oxford University (1987).

[16] Ackland, G.J., Wooding, S.J., and Bacon, D.J., "Defect surface and displacement-threshold properties of alpha-zirconium simulated with a many body potential", *Phil.Mag.A.*, **71**, (1995): 553.

[17] Ackland, G.J., Tichy, G.I., Vitek, V., and Finnis, M.W., "Simple N-body potentials for the noble metals and nickel", *Phil.Mag.A.*, **56**, (1987): 735.

[18] Entel, P., Meyer, R., Kadau, K., Harper, H.C., and Hoffmann, E., "Martensitic transformation: first-principle calculations combines with molecular dynamics simulations", *Eur.Phys.J. B.*, **5**, (1998): 379.

[19] Nishitani, S.R., Kawabe, H., and Aoki, M., "First-principles calculations on bcc-hcp transition of titanium", *Mater.Sci.Eng.A.*, **312**, (2001): 77.

[20] Skriver, H.L., "Crystal structure from one-electron theory", *Phy.Rev.B*, **31** , (1985): 1909.

[21] Mcmahan, A.K., Skriver, H.L., and Johansson, B., "The s-d transition in compressed lanthanum", *Phy.Rev.B*, **23**, (1981): 5016.

[22] Heiming, A., Petry, W., Trampenau, J., Alba, M., Herzig, C., Schober, H.R. , and Vogl, G., "Phonon dispersion of the bcc phase in group-IV metals. II. bcc zirconium, a model case of dynamical precursors of martensitic transitions", *Phy.Rev.B*, **43**, (1991): 10948.

[23] Petry, W., Heiming, A., Trampenau, J., Alba, M., Herzig, C., Schober , H.R., and Vogl, G., "Phonon dispersion of the bcc phase of group-IV metals. I. bcc titanium", *Phy.Rev.B*, **43**, (1991): 10933.

[24] Bogdanoff, P.D., Fultz, B., Robertson, J.L., and Crow, L., "Temperature dependence of the phonon entropy of vanadium", *Phy.Rev.B*, **65**, (2001): 14303.

[25] Dickey, J.M., and Paskin, A., "Computer simulation of the lattice dynamics of solids ", *Phy.Rev*, **188**, (1969): 1407.

[26] Eriksson, O., Wills, J.M., and Wallace, D., "Electronic , quasiharmonic, and anharmonic entropies of transition metals", *Phy.Rev.B*, **46**, (1992): 5221.

[27] Morris, J.R., and Gooding, R.J., "Vibrational entropy effects at a diffusionless first-order solid-to-solid transition", *Phy.Rev.B*, **43**, (1991): 6057.

[28] Morris, J.R., and Gooding, R.J., "Analytic prediction of the exact thermodynamics of a first-order structural phase transition: a practical second order self-consistent phonon theory", *Phy.Rev.B*, **46**, (1992): 8733.

[29] Huang, K., *Statistical Mechanics*, Canada: John Wiley & Sons, (1987).

[30] Kirchhoff, F., Mehl, M.J., Papanicolaou, N.I., Papaconstantopuolos, P.A. , and Khan, F.S., *Dynamical properties of Au from tight-binding molecular dynamics simulations*, preprint, cond-mat:0101168 (January 2001).

[31] Hultgren, R., Desai, R.D., Hawkins, D.T., Gleiser,M., Kelly, K.K., and Wagman, D.D., *Selected Values of the thermodynamics Properties of the Elements*, Metal Park, Ohio: American Society for Metals, (1973).

[32] Persson, K., Ekman, M., and Ozolinŝ, V., "Phonon instability in bcc Sc, Ti, La, and Hf", *Phy.Rev.B*, **61**, (2000): 11221.

[33] Paxton, A.T., Methfessel, M., and Polatoglou, H.M., "Structural energy-volume relations in first-row transition metals", *Phy.Rev.B*, **41**, (1990): 8127.

[34] Stassis, C., Zarestky, J., Mcmasters, O.D., and Harmon, B.N., "Temperature dependence of the normal vibrational modes of hcp Zr" , *Phy.Rev.B*, **18**, (1978): 2632.

[35] Anderson, O.K., "Linear methods in band theory", *Phy.Rev.B*, **12**, (1975): 3060.

[36] Pinsook, U., "Molecular dynamics study of vibrational entropy in bcc and hcp zirconium", *Phy.Rev.B*, **66**, (2002): 24109.

[37] Ahuja, R., Wills, J.M., Johansson, B., and Eriksson, O., "Crystal structures of Ti, Zr, and Hf under compression: Theory", *Phy.Rev.B*, **48**, (1993): 16269.

[38] Srepusharawoot, P., and Pinsook, U., "The bcc-hcp transition temperature in zirconium", *J.Sci.Res.Chula*, **27**, (2002): 131.

[39] Rubini, S., and Ballone, P., "Quasi-harmonic and molecualr dynamics of martensitic transformation in Ni-Al alloys", *Phy.Rev.B*, **48**, (1993): 99.

[40] Pinsook, U.,"Computer simulations of martensitic transition in zirconum" , *Ph.D. Thesis*, The University of Edinburgh (1999).

[41] Pinsook, U., and Ackland, G.J., "Simulation of martensitic microstructural evolution in zirconium", *Phy.Rev.B*, **58**, (1998): 11252.

[42] Pinsook, U., and Ackland, G.J., "Calculation of anomalous phonons and the hcp-bcc phase transition in zirconium", *Phy.Rev.B*, **59**, (1999): 11362.

[43] Kerr, W.C., and Rave, M.J., "Mean-field theory of entropy driven structural phase transition", *Phy.Rev.B*, **48**, (1993): 16234.

[44] Press, W.H., Flannery, B.P., Teukolsky, S.A., and Vetterling,W.T., *Numerical Recipes in C: The Art of Scientific Computing*, Cambridge: Cambridge University Press, (1986).

[45] Mihàly, L., and Martin, M.C., *Solid State Problems and Solutions*, U.S.A.: John Wiley & Sons, (1996).

[46] Osetsky, Y.N., and Serra, A., "Computer-simulation study of high

temperature phase stability in iron", *Phy.Rev.B*, **57**, (1998): 755.

[47] Rahman, A., "Correlations in the motion of atoms in liquid argon", *Phy.Rev.*, **136**, (1964): A 405.

[48] Berendsen, H.J.C., "Biological applications of molecular dynamics " , *Comp.Phys.Commun*, **44**, (1987): 233.

[49] Patra, M., and Karttunen, M., *Molecular Dynamics Simulations of lipid bilayers: Major Artifacts due to Truncating Electrostatic Interactions* , preprint, cond-mat:0211650 (November 2002).

[50] Cong, H.R., Bian, X.F., Li, H., and Wang, L., "Molecular dynamics simulation structure of Cu-Ni alloy ", *Chi.Chem.Phys*, **15**, (2002): 288.

[51] Winkler, A., Horbach, J., Kob, W., and Binder, K., *Structure and Diffusion in amorphous aluminium silicate: A molecular dynamics computer simulation*, preprint, cond-mat:0305227 (May 2003).

[52] Iannuzzi, M., Raiteri, P., Celino, M., and Miglio, L., "Point defects and stacking faults in $TiSi_2$ phase by tight-binding molecular dynamics" , *J.Phys.Cond.Mat*, **14**, (2002): 9535.

[53] Merunka, D., and Rakvin, B., "Molecular dynamics simulation of the soft mode for hydrogen bonded ferroelectrics", *Phys.Rev.B*, **66**, (2002): 174101.

[54] Watson, R.E., and Weinert, M., "Contribution of electronic excitations to the entropy of crystals: the relative stabilities of the hcp, fcc, and bcc structures among the transition metals", *Phys.Rev.B*, **30**, (1984): 1641.

[55] Wang, Y., Ahuja, R., Qian, M.C., and Johansson, B., "Accurate quantum mechanical treatment of phonon instability: body-centred cubic zirconium", *J.Phys.:Condens. Matter.*, **14**, (2002): L695.

[56] Kittel, C., *Introduction to Solid State Physics*, New York: John Wiley & Sons, (1986).

[57] Allen, M.P., and Tildesley, D.J., *Computer simulation of liquids*, Oxford: Clarendon Press, (1987).

Vitae

Mr.Pornjuk Srepusharawoot was born on April 06, 1979 in Burirum. He received a B. Sc. degree in physics from Khonkaen University in 1999.